ARMY RESEARCH LABORATORY

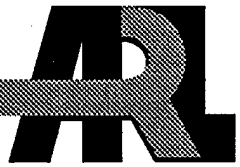

Unusual Laser Excitations (5,890–6,520 Å) of the $B^2\sum^+$ Electronic State of CN in an Atmospheric-Pressure Flame

by J. A. Guthrie, T. S. Bowen, W. R. Anderson,
A. J. Kotlar, and S. W. Bunte

ARL-TR-1381 June 1997

The findings in this report are not to be construed as an official Department of the Army position unless so designated by other authorized documents.

Citation of manufacturer's or trade names does not constitute an official endorsement or approval of the use thereof.

Destroy this report when it is no longer need. Do not return it to the originator.

Army Research Laboratory
Aberdeen Proving Ground, MD 21005-5066

ARL-TR-1381 **June 1997**

Unusual Laser Excitations (5,890–6,520 Å) of the $B^2\sum^+$ Electronic State of CN in an Atmospheric-Pressure Flame

J. A. Guthrie, T. S. Bowen, W. R. Anderson, A. J. Kotlar, S. W. Bunte
Weapons and Materials Research Directorate, ARL

Abstract

The CN radical plays an important role in the chemistry of nitramine propellant flames. Diagnostic methods for detection of this radical are therefore important for studies of its role in propellant combustion experiments. In this work, CN laser induced fluorescence (LIF) in an atmospheric pressure flame was studied. The first such flame study involving observation of LIF in the strong CN B-X violet system, near 3880 Å, but with excitation using strong, fundamental dye laser outputs, near 6000 Å, is reported. Excitation at significantly longer wavelengths (smaller photon energy) than LIF observation wavelengths is unusual. Because the high intensity fundamental outputs of dye lasers may be used, these excitations could ultimately prove to be very effective diagnostic methods for this species. Subsequent investigation of the spectra has revealed that at least four distinct excitation processes, some of which involve molecular collisions, are responsible for the observed LIF as the laser is scanned in this region. The observed spectra reveal some of the unexpected effects of collisions and laser intensity on absorption and fluorescence in this molecule.

TABLE OF CONTENTS

INTENTIONALLY LEFT BLANK.

LIST OF FIGURES

INTENTIONALLY LEFT BLANK.

1. INTRODUCTION

Because of its importance in combustion chemistry, especially in propellant flames, and other fields, the spectroscopy of the cyanide radical has been the subject of intense study for decades [1]. The two strongest and, therefore, best-characterized electronic transitions in CN are the $B^2\Sigma^+-X^2\Sigma^+$ violet system and the $A^2\Pi-X^2\Sigma^+$ red system. The much weaker $B^2\Sigma^+-A^2\Pi$ system was first observed in emission by LeBlanc from the reaction of active nitrogen with various organic molecules [2]. The $B^2\Sigma^+-A^2\Pi$ system is ideally suited to study using laser-induced fluorescence (LIF) spectroscopy because fluorescence in the strong $B^2\Sigma^+-X^2\Sigma^+$ transition is well separated in wavelength from the exciting laser radiation that may be obtained from the fundamental output of common red dyes. This technique has been used to probe the photolysis dynamics of various species containing cyanide and to study interelectronic and intraelectronic collisional energy transfer in CN [3–11]. In these experiments, CN $A^2\Pi$ was generated either by photolysis or reaction of metastable atoms with various cyanides.

The presence of CN $A^2\Pi$ in an atmospheric-pressure flame was demonstrated by Vanderhoff et al. who pumped several $B^2\Sigma^+-A^2\Pi$ transitions using discrete lines of cw ion lasers [12]. The work reported here establishes the viability of this flame as a simple source for at least the $v = 0$ level of CN $A^2\Pi$. This work constitutes the first report of scanned laser excitation of the CN $B^2\Sigma^+-A^2\Pi$ system in a flame and at atmospheric pressure. It also establishes the LIF technique as a suitable diagnostic for CN $A^2\Pi$ in flame environments; this is one of the few cases known in which an electronically excited species, especially a molecular species, has yielded to the LIF technique in a flame environment.

Much weaker, anomalous features were observed interspersed with and to the red of the $B^2\Sigma^+-A^2\Pi$ (0, 0) spectrum. These features have been conclusively identified by comparison with simulated spectra as the CN $A^2\Pi-X^2\Sigma^+$ (8, 3) and (9, 4) bands. Fluorescence in the $B^2\Sigma^+-X^2\Sigma^+$ system can be explained only by interelectronic upconversion from the $A^2\Pi$ state due to collisions in the high-pressure, high-temperature environment. Recordings of fluorescence spectra have firmly identified CN $B^2\Sigma^+$ as the emitter. Although the energy gaps involved are sizable, they are

nevertheless of the order of kT in the flame. A portion of the $A^2\Pi-X^2\Sigma^+$ (10, 5) band has also been recorded near 6,300 Å laser wavelength; $A^2\Pi$, v = 10 is nearly isoenergetic with $B^2\Sigma^+$, v = 0.

Extension of the laser scan to the red of 6,180 Å produces a series of features whose characteristic intensity is an order of magnitude larger than that for the $A^2\Pi-X^2\Sigma^+$ (8, 3) and (9, 4) bands when the laser beam is focused. Analysis has shown that these features are clearly due to two entirely different mechanisms. The first process has been conclusively identified as the simultaneous resonance of the laser with transitions in the overlapping CN $A^2\Pi-X^2\Sigma^+$ (4, 0) and $B^2\Sigma^+-A^2\Pi$ (3, 4) bands assisted by partial rotational relaxation in $A^2\Pi$, v = 4 during the laser pulse. The process may therefore be described as a collision-assisted single-color optical-optical double resonance (OODR) excitation of CN to the $B^2\Sigma^+$ electronic state.

The second process occurring in the same laser-excitation-wavelength range (6,180–6,298 Å) is a newly identified near-resonant two-photon excitation (NR2PE) of CN in the $B^2\Sigma^+-X^2\Sigma^+$ (3, 0) band with $A^2\Pi$, v = 4 providing the intermediate near-resonant levels. Only a few of the strongest features are observable amidst the overlapping OODR spectrum, but their origin is firmly established and has been independently verified in a separate study under near collisionless conditions [13]. The only features observed here are those for which the laser is detuned from a transition in $A^2\Pi-X^2\Sigma^+$ (4, 0) by less than 20 cm^{-1}.

In addition to the aforementioned excitation regions and processes, CN excitation was similarly observed in the region from 6,198–6,520 Å. However, a careful analysis of these features was not attempted. Possible explanations for these excitations is discussed. In addition, spectra in the entire region are presented in Appendix B for possible future study.

Studies of the four assigned excitation processes have been performed only in an atmospheric-pressure flame. Therefore, quantitative information regarding rates of the two collisional mechanisms is not available; the work here described was primarily intended only to identify the mechanisms responsible for producing the observed laser excitation spectra. These processes are

now known; quantification of the relevant transfer rates under more controlled conditions remains for future work. Although the four processes observed are uniquely different in mechanisms, they occur in the same range of laser wavelength, and their resulting spectra are blended. Except for the $B^2\Sigma^+-A^2\Pi$ (0, 0) band, the processes and their associated spectra are unexpected: they appear only due to collisions in the high-pressure flame or because of near-resonance of the laser with certain specific transitions.

2. EXPERIMENTAL

A Nd:YAG-pumped dye laser system (Quantel TDL 60) was operated using the dyes rhodamine 610, rhodamine 640, and DCM to cover the range from 5,890 to 6,520 Å. Typical maximum pulse energies were ≈30 mJ. The laser power was attenuated using neutral density filters. The laser line width was ≈0.07 cm^{-1}, and the pulse duration was ≈10 ns. The beam was either reduced to ≈ 2-mm diameter by an aperture or else focused by a lens (30-cm focal length) into the reaction zone of the flame. The pulse energy was measured using a volume-absorbing disk calorimeter (Scientech 38-0101). The relative laser power during scans was monitored using light scattered from a surface onto a photodiode. Fluorescence was collected perpendicular to the beam by a lens (10-cm diameter), passed through an adjustable iris, filtered, and detected using a photomultiplier tube (EMI 9659QA). A narrow bandpass interference filter (λ_c = 3,864 Å, fwhm = 115 Å) was augmented by one or two broad bandpass colored glass filters (λ_c ≈ 4,000 Å). This combination passed fluorescence (and flame emission) from the CN $B^2\Sigma^+-X^2\Sigma^+$ $\Delta v = 0$ bands. Fluorescence scans were recorded by substituting for the filters and PMT a 0.35 m monochromator (GCA/McPherson EU-700) with a 2,180 line/mm grating and PMT (EMI 9659QA). The fluorescence signals were preamplified (HP 462 A) and processed by a boxcar averager (PAR 162/164). The boxcar output was registered by a strip-chart recorder and also digitized (Metrabyte DAS-16G) and stored on magnetic disk by a microcomputer (Zenith, 80286 microprocessor) for later analysis and printout. The voltage from the photodiode laser-power monitor was digitized and stored in the same way. The curved knife-edge burner employed in these experiments is described in Beyer and DeWilde [14]. Methane (Matheson UHP, 99.97%) and nitrous oxide (Matheson CP, 99.0%) were premixed and undiluted, the

equivalence ratio being $\phi \approx 2.4$ ($\phi = 4[CH_4]/[N_2O]$). The gas flow rates were controlled by manual metering valves. Previous work has shown that the plateau temperature obtained in the reaction zones of various flames using this burner is very near the adiabatic flame temperature [14, 15], approximately 2,300 K at $\phi \approx 2.4$.

3. RESULTS AND DISCUSSION

As noted in section 1, laser excitation of CN near 6,000 Å in an atmospheric-pressure flame produces the $B^2\Sigma^+$ electronic state by four independent processes (See Figures 1a–1c): (1) absorption in the $B^2\Sigma^+-A^2\Pi$ (0, 0) band; (2) absorption in the $A^2\Pi-X^2\Sigma^+$ (8, 3), (9, 4), and (10, 5) bands followed by collisional interelectronic conversion from $A^2\Pi$ to $B^2\Sigma^+$; (3) a collision-assisted single-color OODR via $A^2\Pi-X^2\Sigma^+$ (4, 0) and $B^2\Sigma^+-A^2\Pi$ (3, 4); and (4) a NR2PE in the $B^2\Sigma^+-A^2\Pi$ (3, 0) band via intermediate $A^2\Pi$, v = 4 rotational levels. These four processes and the region from 6,298–6,520 Å are discussed separately.

3.1 CN $B^2\Sigma^+-A^2\Pi$ (0, 0) Band. The excitation/fluorescence process for the CN $B^2\Sigma^+-A^2\Pi$ (0, 0) band is depicted schematically in Figure 1a. Part of the excitation spectrum recorded in the flame is shown in Figure 2. The spectrum has been normalized with respect to laser power. The beam was not focused, and the laser pulse energy was ≈0.05 mJ so that the spectral irradiance was $I_\nu \approx 2 \times 10^6$ W/cm^2 cm^{-1}.* Transition wavelengths were computed using molecular constants from Kotlar et al. [16] and from Engleman [17]. The band with line assignments extended to 5,890 Å may be found in Appendix A. For comparison, a $B^2\Sigma^+-A^2\Pi$ (0, 0) band excitation scan obtained following flash photolysis of cyanogen to produce CN $A^2\Pi$ may be found in Conley et al. [10]. The results are in essential agreement.

Efforts to deduce an effective rotational temperature for CN $A^2\Pi$, v = 0 from excitation scans like that shown in Figure 2, were thwarted by two related experimental difficulties. (1) The

* The spectral irradiance is calculated here as pulse energy/pulse duration × line width. Note, that to make this definition appropriate for multiplication by the Einstein B coefficient, one must take care to divide by 4π or by the speed of light, depending upon whether B is expressed in terms of isotropic intensity or energy density, respectively.

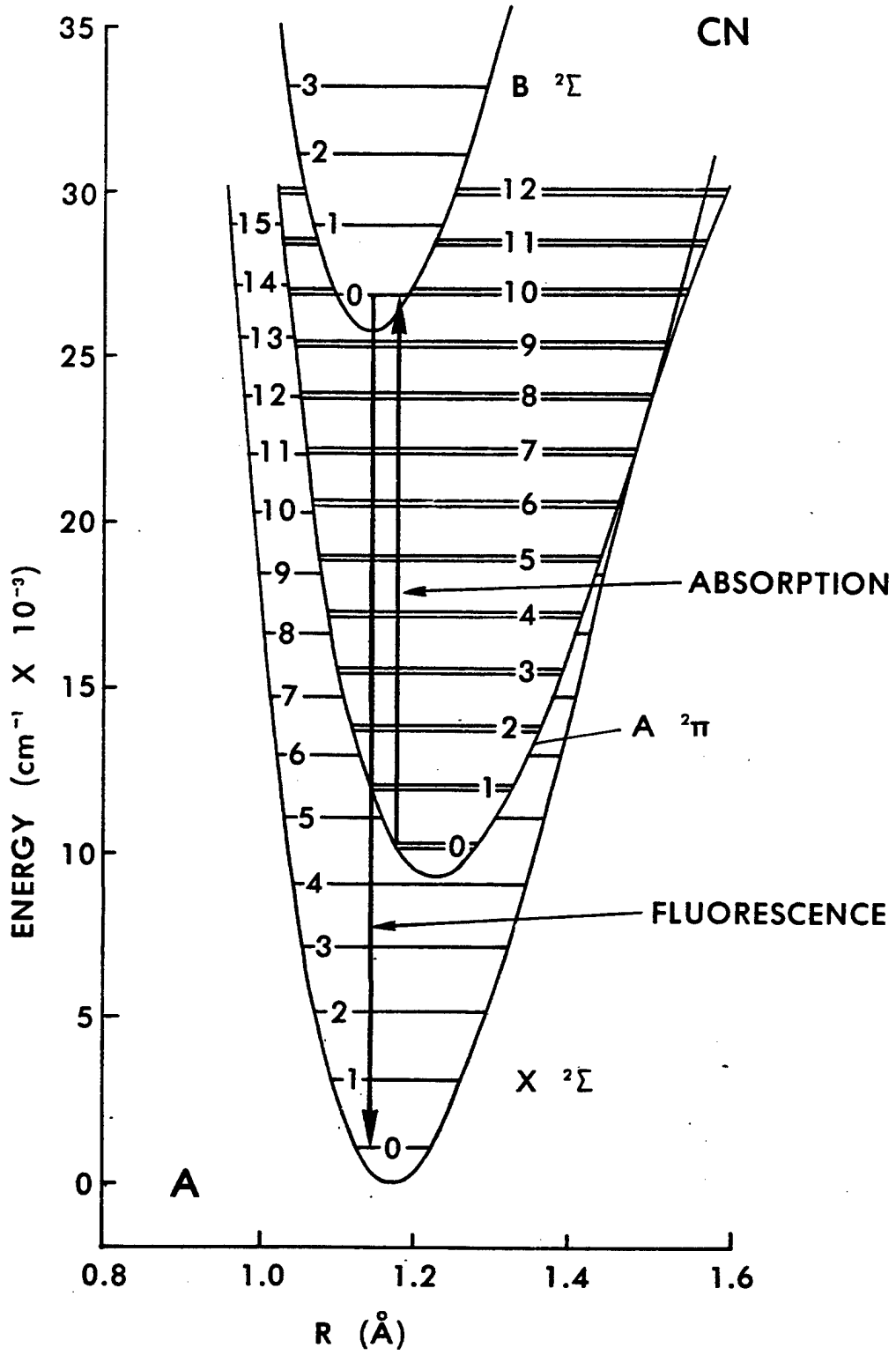

Figure 1a. Mechanism (a) for producing $B^2\Sigma^+$ state CN in the flame: absorption in the $B^2\Sigma^+ - A^2\Pi$ (0, 0) band.

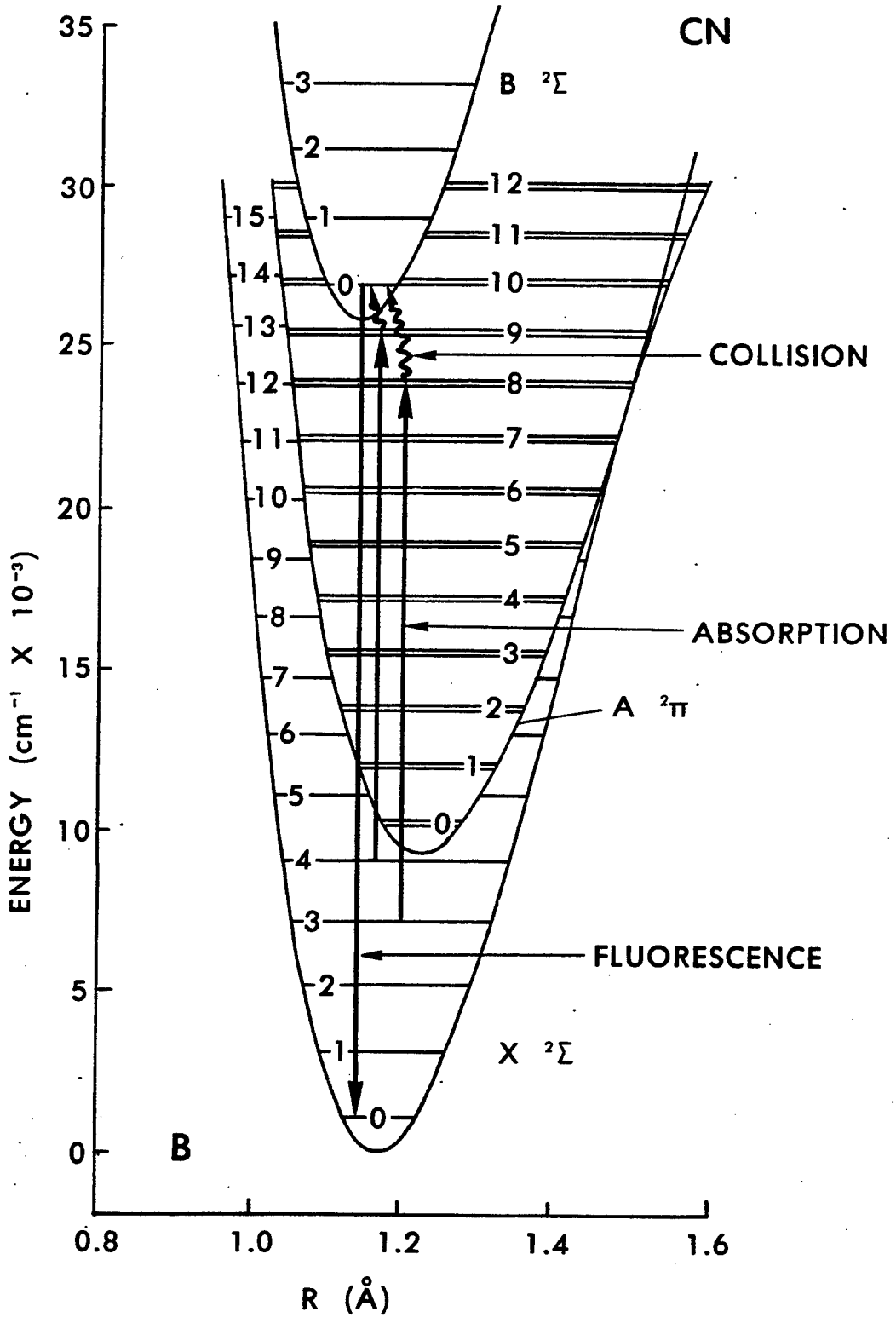

Figure 1b. Mechanism (b) for producing $B^2\Sigma^+$ state CN in the flame: absorption in the $A^2\Pi - X^2\Sigma^+$ (8, 3) and (9, 4) bands followed by collisional interelectronic conversion to $B^2\Sigma^+$.

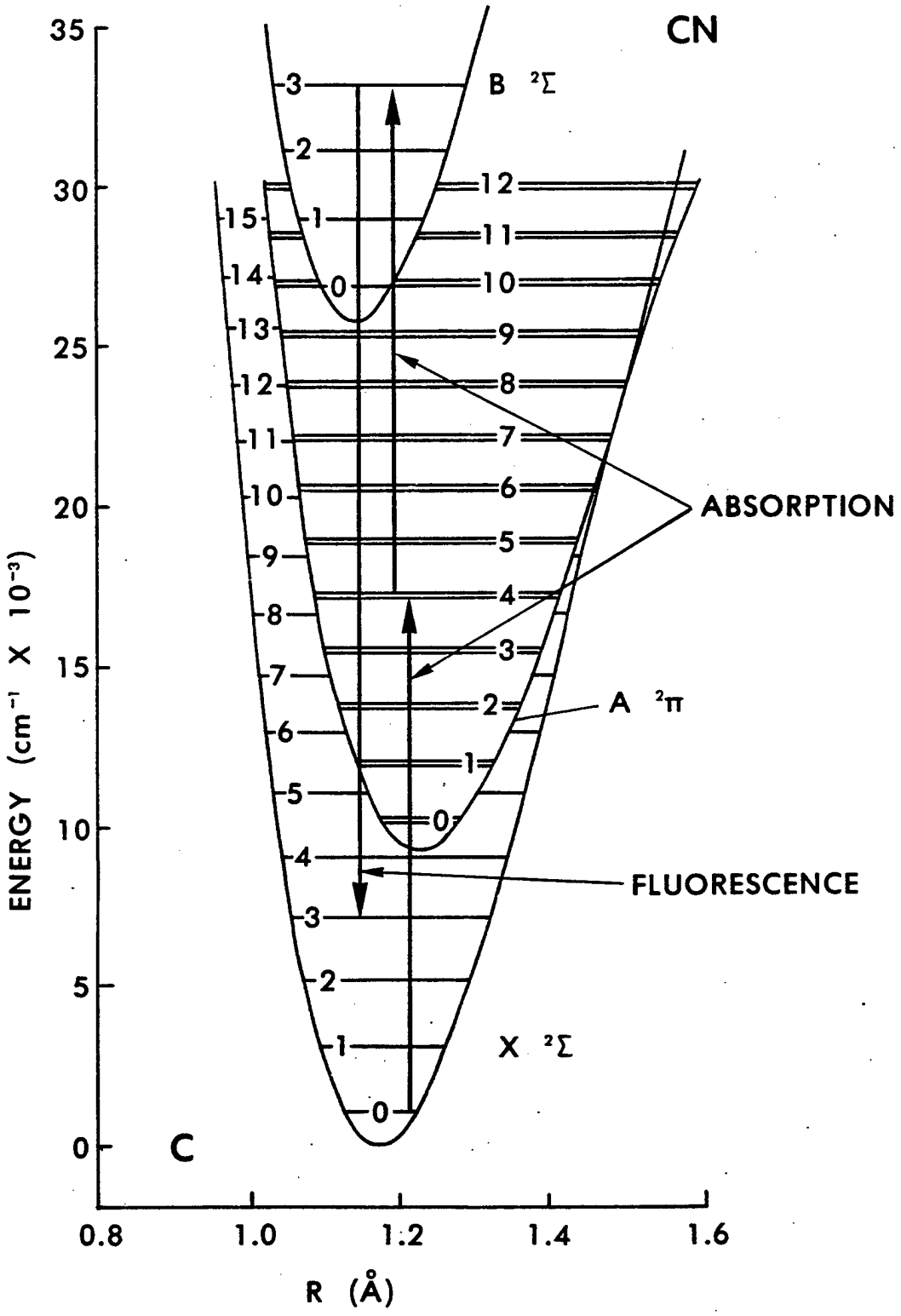

Figure 1c. Mechanism (c) for producing $B^2\Sigma^+$ state CN in the flame: collision-assisted single-color optical-optical double resonance transitions via the $A^2\Pi - X^2\Sigma^+$ (4, 0) and $B^2\Sigma^+ - A^2\Pi$ (3, 4) bands. A near-resonant two-photon excitation also occurs in the same wavelength region (see text).

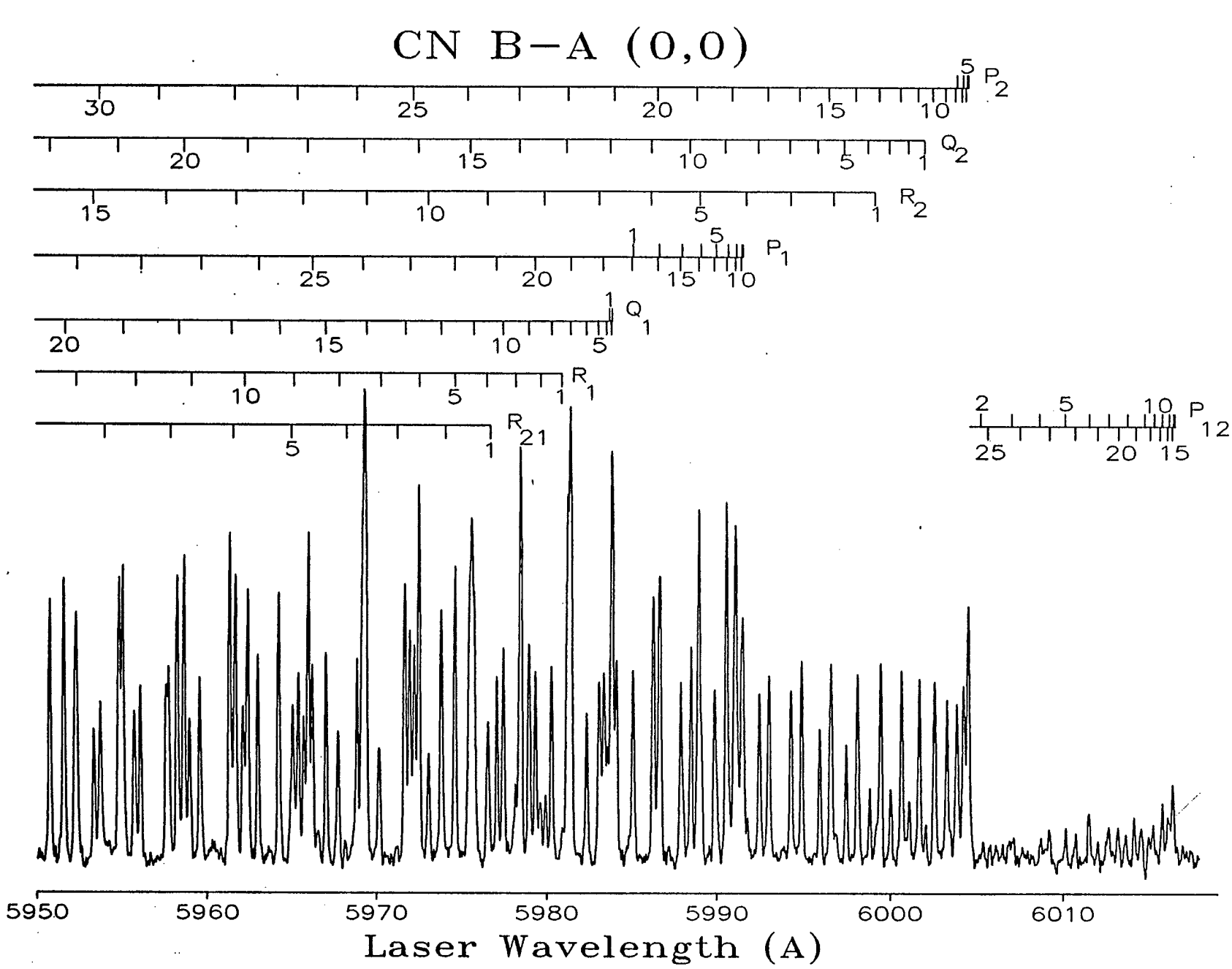

Figure 2. CN $B^2\Sigma^+$–$A^2\Pi$ (0, 0) band excitation spectrum in an atmospheric-pressure CH_4/N_2O flame.

nascent CN $B^2\Sigma^+$ in the flame emits within the filter bandpass, thereby producing a noisy background. The S/N ratio degrades rapidly with decreasing laser power. The emission also loads the PMT requiring care to avoid its saturation in detecting the LIF. (2) In practice, it was found that partial saturation of these transitions was easily obtained in spite of the relatively small oscillator strength for the band ($\approx 4 \times 10^{-4}$) [11, 18]. Use of an unfocused beam (in order to avoid saturation) promotes sampling of sizable spatial regions. The temperature may vary substantially over these regions in the atmospheric-pressure flame. At this time, the rotational temperature of $A^2\Pi$, v = 0 in the flame, if one can be determined, remains unknown.

In addition to these known difficulties, there also exists the possibility of contamination of the fluorescence signals by another mechanism; weak features may be present among the strong $B^2\Sigma^+-A^2\Pi$ (0, 0) lines. These features are due to the collisional process discussed in section 3.2. The weaker peaks may be obscured by saturation broadening the $B^2\Sigma^+-A^2\Pi$ lines when a powerful laser, such as the YAG-pumped dye system used for the present study, excites the LIF. If collisions are possible, the presence of these features could affect the results of quantitative LIF measurements even when the source of CN is, for instance, photolysis of a stable precursor.

3.2 CN $A^2\Pi-X^2\Sigma^+$ (8, 3), (9, 4) and (10, 5) Bands. The anomalous features appearing in the $B^2\Sigma^+-A^2\Pi$ (0, 0) band are most clearly seen among the weak lines of the P_{12} branch near 6,006 Å in Figure 2. (Also see an expanded view in Appendix A.) These weak features, extending from 6,016 to 6,100 Å, are shown as the lower trace in Figure 3 and, as indicated there, have been conclusively identified as the $A^2\Pi-X^2\Sigma^+$ (8, 3) band. The upper trace in Figure 3 is a simulated spectrum computed from the constants of Kotlar [16] assuming a flame temperature of 2,300 K. The laser beam was unfocused, yielding a spectral irradiance of $\approx 6 \times 10^7$ W/cm^2 cm^{-1}. Further to the red, the $A^2\Pi-X^2\Sigma^+$ (9, 4) band is also excited by the laser with fluorescence detected near 3,860 Å. Figure 4 shows the spectrum recorded from 6,130 to 6,180 Å and a simulation of the overlapping $A^2\Pi-X^2\Sigma^+$ (8, 3) and (9, 4) bands. Only the main (9, 4) branches have been assigned in Figure 4. As can be seen from Figure 3, the $A^2\Pi-X^2\Sigma^+$ (8, 3) band extends well into the $B^2\Sigma^+-A^2\Pi$ (0, 0) band, as far as the R_{21} branch head at 5,983.76 Å. With sufficiently high S/N the $A^2\Pi-X^2\Sigma^+$ (7, 2) band, which extends further to the red, might also be observed.

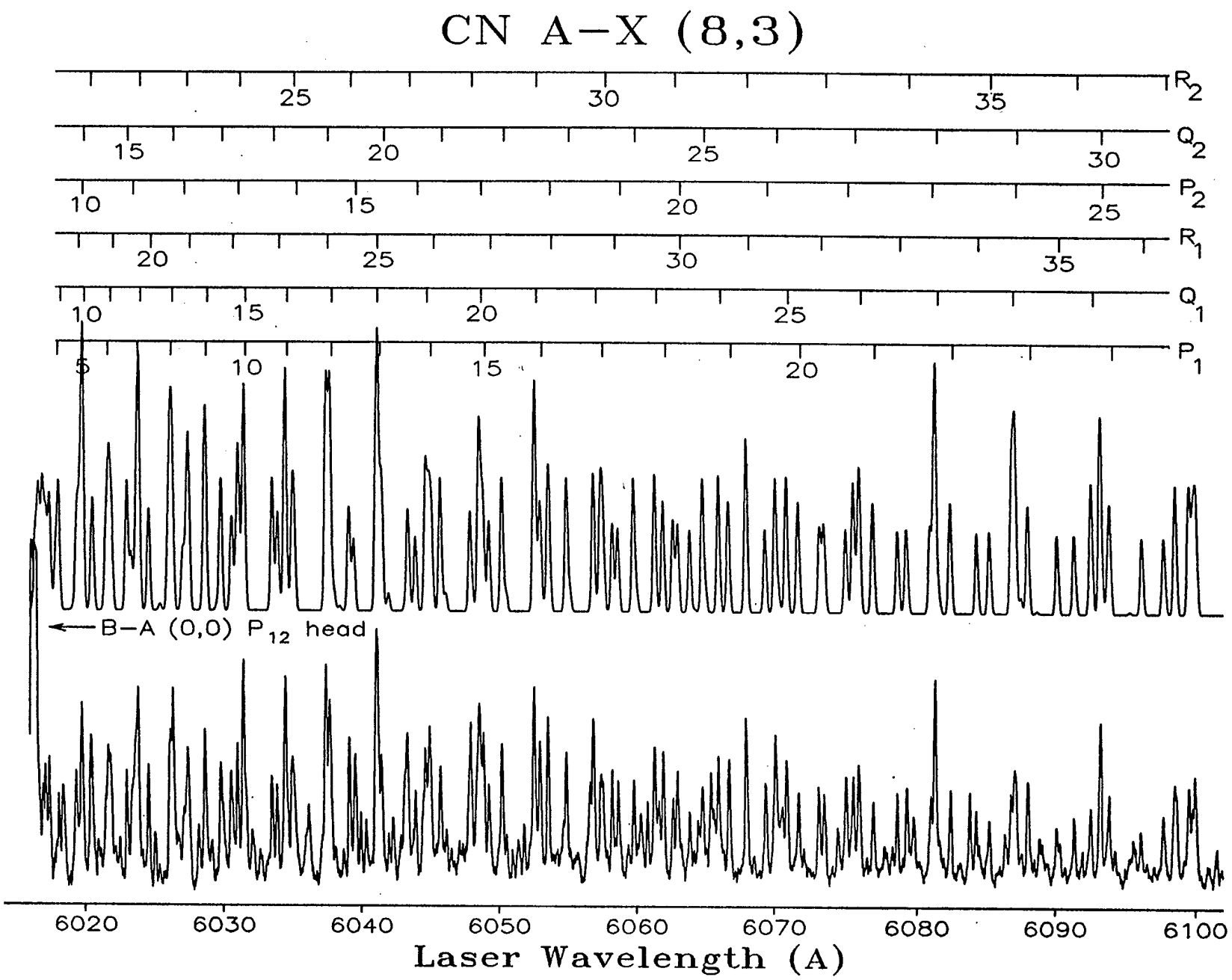

Figure 3. CN $A^2\Pi$–$X^2\Sigma^+$ (8, 3) band excitation spectrum with $I_v \simeq 6 \times 10^7$ W/cm$^2 \cdot$ cm^{-1} (lower trace).

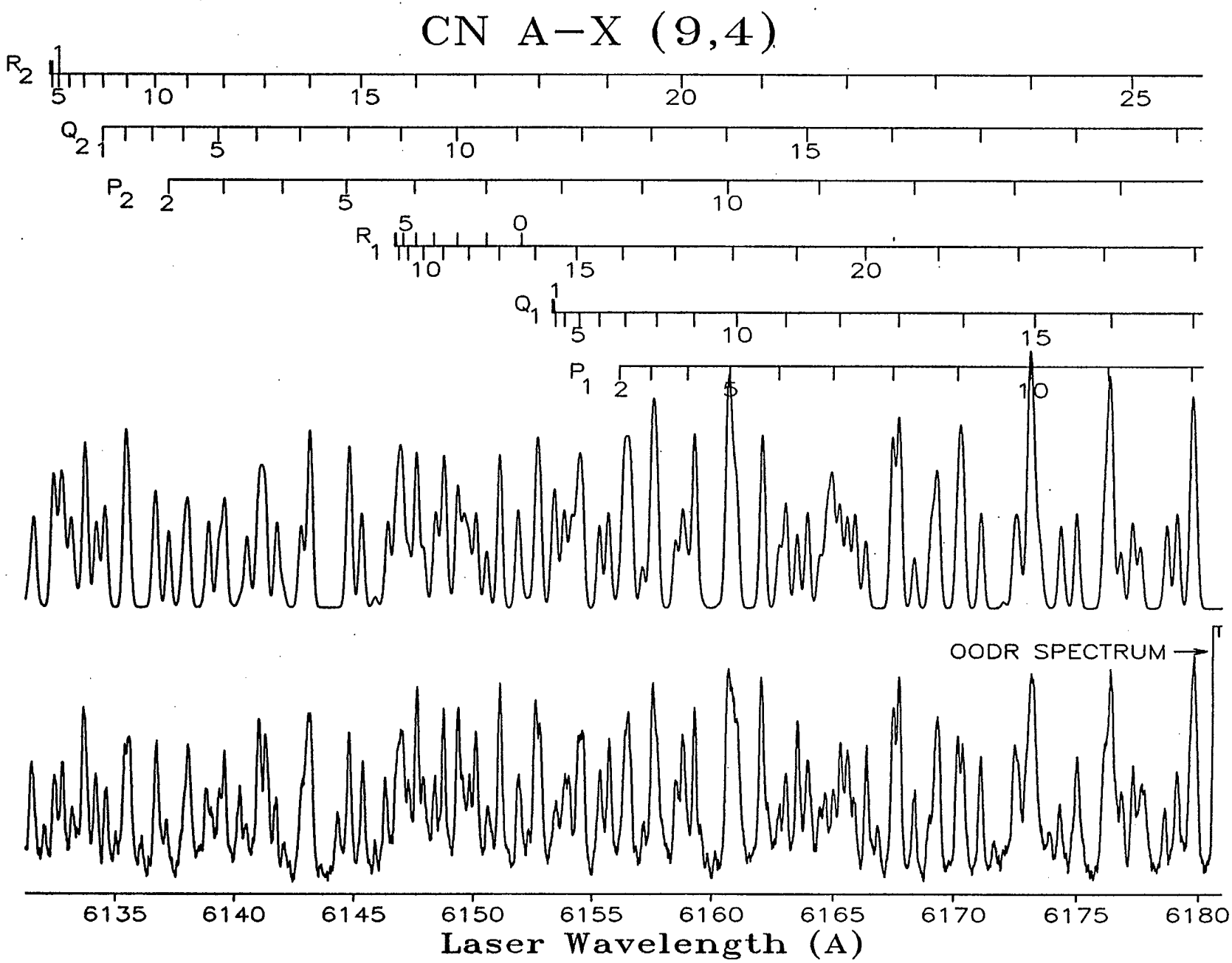

Figure 4. Overlapping CN $A^2\Pi$–$X^2\Sigma^+$ (8, 3) and (9, 4) excitation spectra with $I_v \approx 6 \times 10^7$ W/cm$^2 \cdot$ cm^{-1} (lower trace).

The observation of the $A^2\Pi-X^2\Sigma^+$ (8, 3) and (9, 4) bands by fluorescence in the $B^2\Sigma^+-X^2\Sigma^+$ $\Delta v = 0$ sequence can be attributed only to interelectronic conversion of $A^2\Pi$, v = 8 and 9 to $B^2\Sigma^+$ by endoergic collision with hot-flame molecules, as illustrated in Figure 1b. The populations in the v = 3 and 4 levels of the $X^2\Sigma^+$ state relative to the total electronic state population are 2.1×10^{-2} and 6.8×10^{-3}, respectively, assuming a thermal vibrational distribution at 2,300 K. The energy gaps between the rotationless $B^2\Sigma^+$, v = 0–$A^2\Pi$, v = 8 and $B^2\Sigma^+$, v = 0–$A^2\Pi$, v = 9 levels are 3,097 and 1,516 cm^{-1}, respectively, while kT = 1,598 cm^{-1} at 2,300 K. The smaller energy deficit for $A^2\Pi$, v′ = 9 relative to v′ = 8 is offset by the fact that it is populated by pumping from a vibrational level with lower population (assuming thermal equilibrium). The (8, 3) and (9, 4) bands have approximately the same oscillator strengths [19].

Attempts to record excitation spectra of the (8, 3) and (9, 4) bands by detecting fluorescence in the $A^2\Pi-X^2\Sigma^+$ (8, 4), (8, 2), (9, 5), and (9, 3) bands near 6,806, 5,363, 6,974, and 5,483 Å, respectively, were not successful. These bands are among the strongest in the red system having v′ = 8 and 9 [19]. The fact that fluorescence was observed in the $B^2\Sigma^+-X^2\Sigma^+$ (0, 0) band, but not in the strongest $A^2\Pi-X^2\Sigma^+$ bands with v′ = 8, 9, reflects in part the higher sensitivity of the PMT (a factor of 2–3) in the near ultraviolet (UV) as opposed to the red, but results primarily from an oscillator strength for the $B^2\Sigma^+-X^2\Sigma^+$ transition, which is ≈40 times larger than the relevant transitions in $A^2\Pi-X^2\Sigma^+$ [19]. Confirmation of $B^2\Sigma^+$ as the emitting state was obtained by recording the fluorescence spectrum shown in Figure 5. The spectrum was obtained while pumping the strong feature in the (9, 4) band at 6,160 Å, an unresolved set of lines from several branches. The fluorescence spectrum is unquestionably identified as that of the $B^2\Sigma^+-X^2\Sigma^+$ transition.

The $A^2\Pi-X^2\Sigma^+$ (10, 5) band was also observed near 6,300 Å. Collisional conversion of CN to $B^2\Sigma^+$, v = 0 following laser excitation of $A^2\Pi$ v = 10 has been reported previously in 2 torr of argon at 300 K [20]. Because $A^2\Pi$, v = 10 and $B^2\Sigma^+$, v = 0 are approximately isoenergetic, nearly elastic collisions with flame molecules, can induce the intermolecular conversion. In this report, strongly enhanced fluorescence was observed (more clearly, under unsaturated conditions)

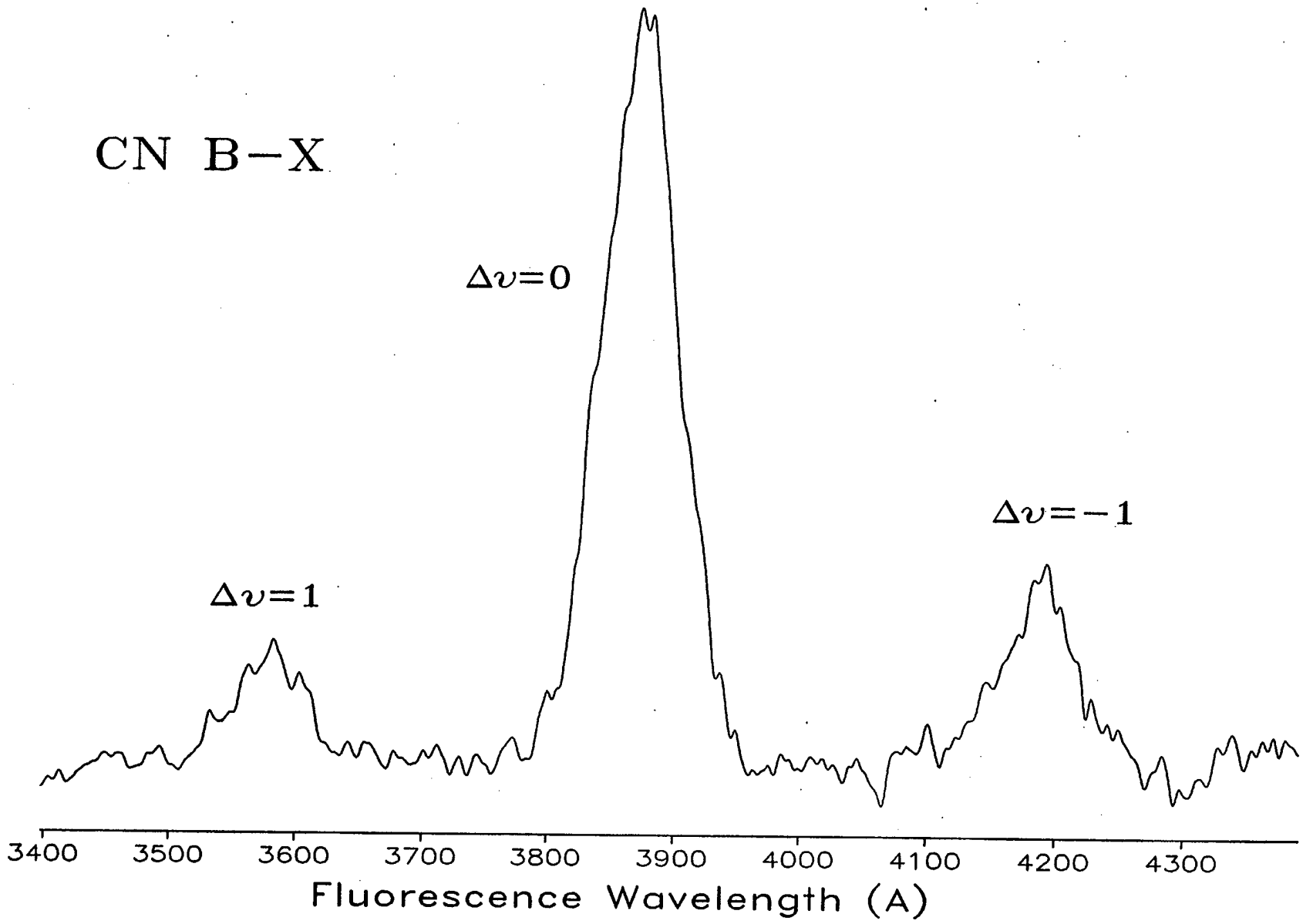

Figure 5. Low-resolution LIF spectrum observed while pumping the unresolved feature in the $A^2\Pi - X^2\Sigma^+$ (9, 4) band at 6,160.86 Å.

on the perturbed and extra $Q_2(16)$ lines at 6,315.44 and 6,316.07 Å, respectively. A portion of the (10, 5) band excitation spectrum containing these lines appears as the inset in Figure 6. The inset spectrum was recorded with the laser unfocused ($I_v \approx 8 \times 10^7$ W/cm^2 cm^{-1}). The perturbation and intensity enhancement in $A^2\Pi$, v = 10 at J = 15.5 is well known [21]. Calculations using the methods outlined by Kotlar et al. [16] indicate that the perturbed and extra J = 15.5 levels have 10.5% and 89.5% sigma character, respectively. The interelectronic conversion from perturbed rotational levels is collisionless and very rapid [20]. Therefore, the ratio E/Q of the rate of electronic conversion to that for quenching is greater than E/Q for the unperturbed levels, which require collisions to promote the conversion. Hence, the fluorescence quantum yield from $B^2\Sigma^+$, v = 0 is enhanced for the perturbed levels. Unidentified features were found mixed with the (10, 5) lines. Because of this congestion, a full assignment of the (10, 5) band was not attempted. The unidentified lines may belong to one of several possible $B^2\Sigma^+$–$A^2\Pi$ $\Delta v = -1$ bands which have transitions near 6,300 Å [19]. Features which remain unidentified were recorded in laser excitation scans extending to 6,520 Å. (See section 3.5 and Appendix B.)

It should be explicitly emphasized that the observed spectra cannot be due to UV fluorescence in $A^2\Pi$–$X^2\Sigma^+$ bands with v′ = 8, 9, or 10. All fluorescence from $A^2\Pi$, v′ = 8, 9 is rejected by the filters in the detection system. Only the $A^2\Pi$–$X^2\Sigma^+$ (10, 0) band could conceivably be detected in fluorescence; however, the oscillator strength for this transition, as for all UV $A^2\Pi$–$X^2\Sigma^+$ transitions, is vanishingly small [19]. Figure 5 provides incontrovertible proof that the emitter is $B^2\Sigma^+$. Figure 5 also shows that there is clearly fluorescence in at least one $\Delta v = +1$ band of the $B^2\Sigma^+$–$X^2\Sigma^+$ transition. This observation is possible only if the collisional uptransfer processes also populate $B^2\Sigma^+$, v > 0. The same result was observed when pumping $^2\Sigma^+ > A^2\Pi$–$X^2\Sigma^+$ (8, 3) transitions. Collisional interelectronic conversion from $A^2\Pi$, v = 8, 9 to $B^2\Pi^+$, v>0 even at 2,300 K is totally unexpected given the magnitude of the energy gaps involved. In addition, although Figure 1b shows a direct production of $B^2\Sigma^+$, v = 0 from $A^2\Pi$ v = 8, 9, it is entirely possible that multistep collisional mechanisms involving distribution of population into high-lying vibrational levels of both $A^2\Pi$ and $X^2\Sigma^+$ and, thence, to $B^2\Sigma^+$, could contribute in large part to the observed fluorescence. Rapid collisional equilibration of

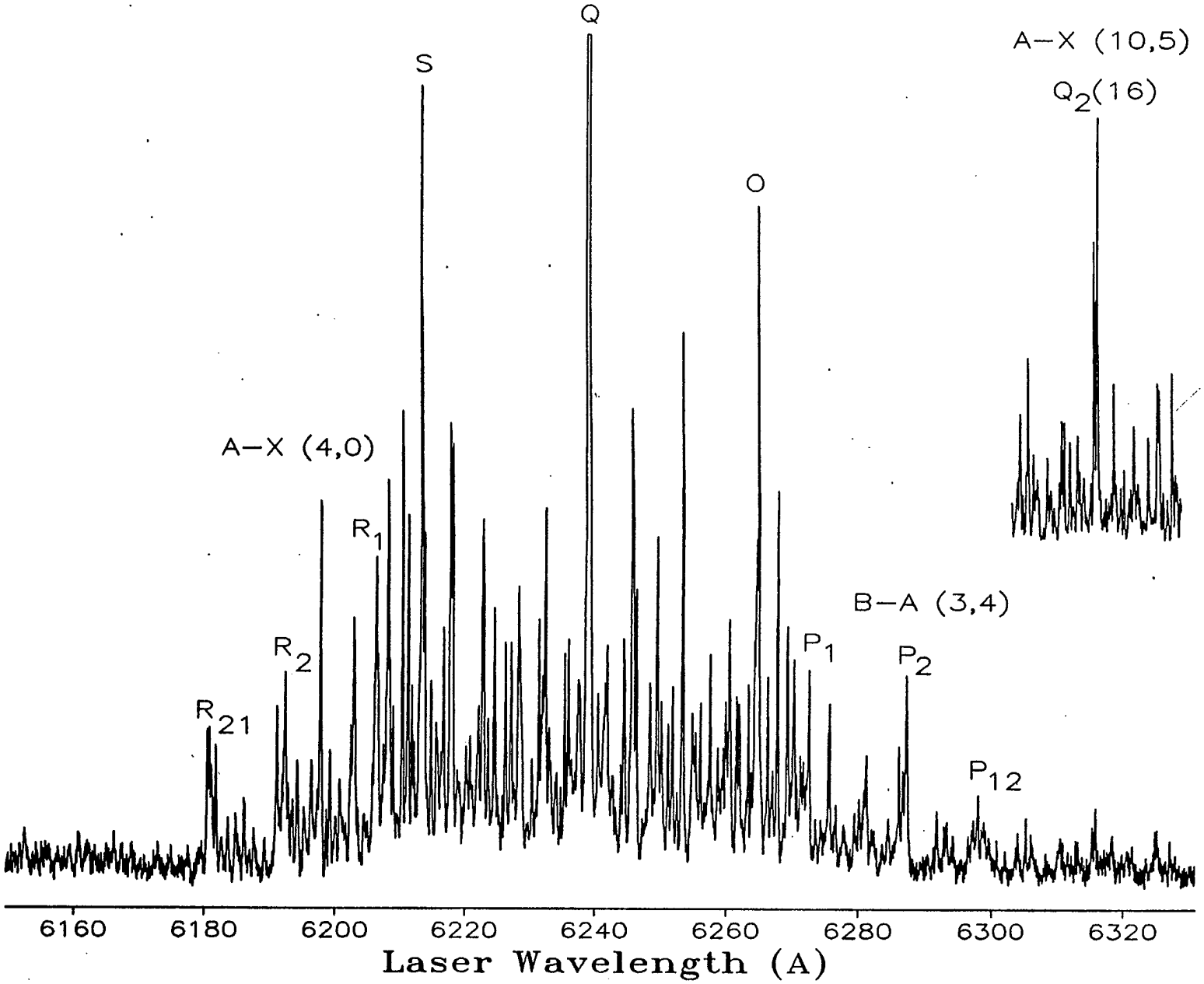

Figure 6. Laser-induced excitation spectrum observed between 6,160 and 6,320 Å with the laser focused to give $I_v \approx 9 \times 10^{10}$ W/cm$^2 \cdot$ cm^{-1}.

population in nearly resonant vibrational levels of the electronic states of CN in a few torr of argon is well established [4–9, 20, 22].

3.3 Collision-Assisted Single-Color OODR via $A^2\Pi-X^2\Sigma^+$ (4, 0) and $B^2\Sigma^+-A^2\Pi$ (3, 4) Bands. With increasing laser wavelength and the beam focused in the flame ($I_v \approx 9 \times 10^{10}$ W/cm^2 cm^{-1}) the weak spectra due to $A^2\Pi-X^2\Sigma^+$ (8, 3) and (9, 4) give way to a much stronger series of peaks beginning at about 6,180 Å (see Figure 6). The strong peaks extend to about 6,283 Å, then the spectrum abruptly returns to much weaker features as the wavelength increases. It is to be emphasized that the weak features outside this region are not noise; they are also LIF peaks (see Figure 4). The mechanism producing the intense features becomes clear when it is realized that (1) 6,180 Å corresponds to the (R_{21}) head of the red-degraded $A^2\Pi-X^2\Sigma^+$ (4, 0) band; (2) 6,283 Å corresponds to the (P_2) head of the blue-degraded $B^2\Sigma^+-A^2\Pi$ (3, 4) band; and (3) the upper vibronic level for the first band ($A^2\Pi$, v = 4) is the lower vibronic level for the second. The intense features are limited to the wavelength region in which the $A^2\Pi-X^2\Sigma^+$ (4, 0) band overlaps the $B^2\Sigma^+-A^2\Pi$ (3, 4) band. Four of the branch heads expected for one-photon excitation of the $A^2\Pi-X^2\Sigma^+$ (4, 0) and $B^2\Sigma^+-A^2\Pi$ (3, 4) bands are clearly well developed in the OODR spectrum. These are identified in Figure 6, along with others which do not appear so clearly; the P_{12} head is the furthest red feature in the $B^2\Sigma^+-A^2\Pi$ (3, 4) band. Therefore, the strong features recorded in the range 6,180–6,283 Å must result from single-color OODRs in $A^2\Pi-X^2\Sigma^+$ (4, 0) and $B^2\Sigma^+-A^2\Pi$ (3, 4). As will be discussed, the density of features in this range can be explained only by acknowledging the effects of significant rotational relaxation in $A^2\Pi$, v = 4 during the laser pulse.

Figure 7 shows the laser-induced excitation spectrum of the $A^2\Pi-X^2\Sigma^+$ (4, 0) band recorded by detecting fluorescence in the $A^2\Pi-X^2\Sigma^+$ (4, 1) band near 7,100 Å. Line assignments were made using spectral constants from Kotlar et al. [16]. The lower trace in Figure 7 is the corresponding UV fluorescence obtained with the monochromator set at 3,860 Å, as in Figure 6. Inspection of the two traces shows, with a few exceptions, that for each peak in the UV fluorescence scan, there is one at the same wavelength in the upper trace. There can be no doubt that the $A^2\Pi-X^2\Sigma^+$ (4, 0) band is involved in production of the UV fluorescence. The extremely irregular variation in the peak intensities is to be expected for single-color OODRs in a

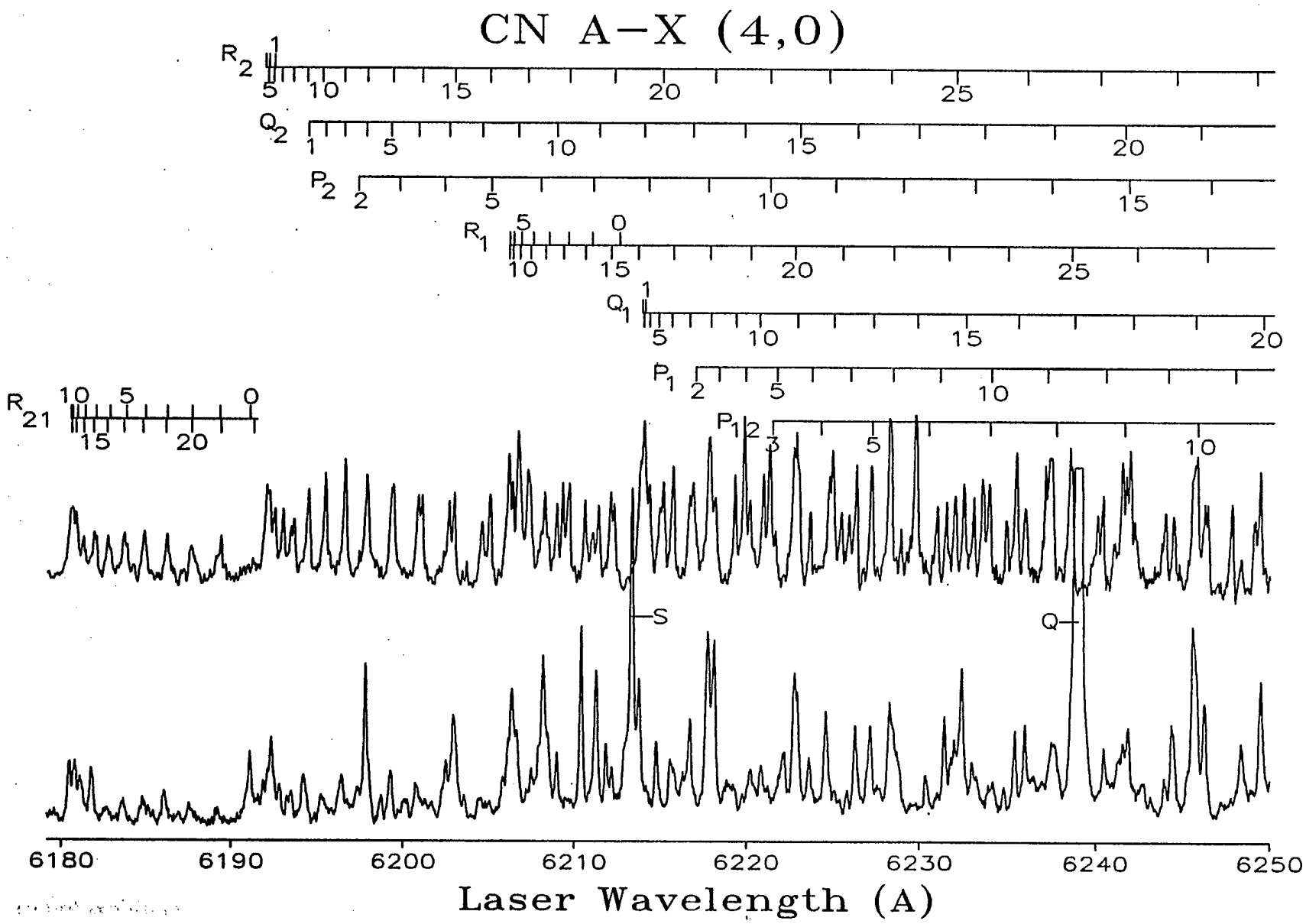

Figure 7. $A^2\Pi$–$X^2\Sigma^+$ (4, 0) band excitation spectrum recorded by detecting fluorescence in the $A^2\Pi$–$X^2\Sigma^+$ (4, 1) band near 7,100 Å (upper trace), and the single-color OODR spectrum observed in fluorescence near 3,860 Å (lower trace).

collisional environment, such as a flame, as will be discussed more fully. Measurements of the fluorescence signal as a function of laser power (focused) on a number of the stronger features yielded power dependencies less than unity, indicating at least partial saturation of both OODR transitions. The spectra shown in Figures 6 and 7 were recorded with $I_v \approx 9 \times 10^{10}$ W/cm^2 cm^{-1}. The features in Figures 6 and 7, labeled S, Q, and O, are due to the NR2PE process discussed in section 3.4.

The number of single-color OODR transitions possible in direct collision-free excitations via the $A^2\Pi$-$X^2\Sigma^+$ (4, 0) and $B^2\Sigma^+$-$A^2\Pi$ (3, 4) bands is less than 10, assuming a saturation-broadened linewidth for both transitions of $\approx$1 cm^{-1}. Therefore, the richness of the spectrum in Figure 6 can be explained only by invoking rapid rotational relaxation in $A^2\Pi$, v = 4 during the 10 ns laser pulse. This process allows rotational levels neighboring the one initially populated by absorption of the first photon to serve as lower levels for the second absorption. Note that a typical mean time for LIF quenching collisions to occur in atmospheric-pressure flames is of the order of 1 ns, 10 times shorter than the laser pulse; rotational relaxation typically occurs about five times faster [23, 24]. The production of the OODR features through collisions has been confirmed in a separate study at low pressures [13]. At 0.2 torr of cyanogen, only the NR2PE lines appear in the laser excitation spectrum. When the pressure is raised to 1.0 torr, new features arise that can be directly matched with those observed in the atmospheric-pressure flame.

The rotational population distribution of a molecule that has been excited by a laser in a collisional environment, such as a flame, is generally strongly peaked about the originally pumped level during and immediately after the laser pulse, but with very significant population in nearby rotational levels [23, 24]. Although the distributions generally fall off rapidly as one moves away from the originally pumped level, there are usually a large number of rotational levels exhibiting significant population. The observed distributions are the result of competition between rotational relaxation collisions, the laser excitation process, and the combined effects of electronic quenching and vibrational relaxation collisions. The first process tends to bring about

rotational equilibration within the excited vibrational level; the latter three tend to preserve peaking of the rotational distribution about the level pumped by the laser. At atmospheric pressure, collisional rates are generally much faster than radiative emission so that emission has negligible effect on the excited-state distribution. The rotational distribution changes with time, but it is nevertheless generally strongly peaked at the pumped level during the laser pulse. Rotational equilibration of the excited state typically occurs some time after the pulse, as nicely demonstrated in an experiment on OH $A^2\Sigma^+$ by Stepowski and Cottereau in a low-pressure flame ($\approx$20 torr) [25].

The typical situation in atmospheric-pressure flames is somewhere between two hypothetical limiting cases [23, 24]: (1) the so-called "frozen excitation" limit, wherein the vibrational and quenching collisions completely dominate rotational relaxation, resulting in observation of only the originally pumped level; and (2) the completely rotationally relaxed limit, which would occur if rotational transfer collisional rates dominated the other effects. It is worthwhile to reiterate that the mean time between quenching collisions ($\approx$1 ns) is typically about five times longer than that for rotational transfer collisions. It is therefore very reasonable to assume that incomplete, but significant, rotational relaxation occurs in the $A^2\Pi$, v = 4 level of CN during the laser pulse in the present experiments. Incomplete rotational relaxation of CN $B^2\Sigma^+$ in competition with quenching and vibrational transfer in a similar flame has been demonstrated in cw laser experiments [15]. The excited-state rotational distribution upon ion laser excitation of several levels in C_2 $d^3\Pi_g$, CN $A^2\Pi$, and CN $B^2\Sigma^+$ exhibits the same characteristics [26].

Analysis has shown that the observed OODR transition wavelengths correspond overwhelmingly to simultaneous resonances in both $A^2\Pi$–$X^2\Sigma^+$ (4, 0) and $B^2\Sigma^+$–$A^2\Pi$ (3, 4) assuming rotational relaxation in $A^2\Pi$, v = 4 and a saturation-broadened linewidth of 0.7 cm^{-1}. A detailed simulation of the OODR spectrum is, in principle, possible. However, it would be a decidedly nontrivial task, particularly with regard to reproducing the observed intensities. The following effects must be included. (1) The rotational distribution in the intermediate level ($A^2\Pi$, v = 4) is not expected to be at either of the limits mentioned in the preceding paragraph, and the distribution is expected to be time-dependent during the laser pulse. Little information exists

regarding rate parameters for CN in this state and colliders in the flame, particularly at high temperature. (2) Transition wavelengths for the two single-photon transitions involved in each OODR transition must be very well known. The overlap of the one-photon transitions strongly affects the expected intensity. It is easily shown that such overlaps are very sensitive to slight errors in the transition wavelengths. (3) Line shapes strongly affect the overlap calculations. The line shapes are not well known since they are affected by both collisions and saturation. (4) Saturation of transitions will affect intensities through depletion of the lower rotational level in a collisional environment [23, 24]. The relative strength of the effect depends on rotational levels involved in the transition, line strengths, colliders, and temperature. (5) The linestrengths of each one-photon transition involved must also be included; unlike the other information required, these are well known. A number of the preceding effects represent major efforts to model in themselves, in particular the first and fourth. Because of the large uncertainties in many of these parameters, the value of a detailed simulation appears doubtful. A simulation closely approaching this level of complexity has been carried out for an identical mechanism known to occur in Li_2 (at 4 torr and using a cw dye laser) with only moderately successful results, indicating the difficulty of the calculation [27, 28]. Variability in these many effects among the lines in the OODR spectrum produces their irregular intensities.

3.4 NR2PE in the $B^2\Sigma^+-X^2\Sigma^+$ (3, 0) Band. Certain features in the OODR region, particularly those labeled S, Q, and O in Figure 6, were recognized as problematic if due to this collision-assisted process because their large intensities could not be readily explained. The (offscale) peak, labeled Q, is three times larger than the next most intense peak (S) when the beam is focused to give $I_v \approx 9 \times 10^{10}$ W/cm^2 cm^{-1}. It was then noted that the wavelength of the offscale peak corresponds to half the energy of the $B^2\Sigma^+-X^2\Sigma^+$ (3, 0) band origin, which suggested the peak might be the Q-branch head of a nonresonant two-photon absorption in this band. Further analysis and experiments have confirmed this assignment. Although the Franck-Condon factor for this transition is exceedingly small ($\approx 2 \times 10^{-5}$) [19], the two-photon transition rate is significantly enhanced by near-resonances with rotational levels of $A^2\Pi$, v = 4. Because the collision-assisted OODR features obscure most of the lines of the two-photon $B^2\Sigma^+-X^2\Sigma^+$

(3, 0) band, the spectrum has recently been recorded at low pressure in CN produced by photolysis of C_2N_2. The simplified spectrum and its analysis may be found in Guthrie et al. [13].

The rotational constants for $B^2\Sigma^+$, $v' = 3$ and $X^2\Sigma^+$, $v'' = 0$ differ by only $\approx 3 \times 10^{-3}$ cm^{-1} [16, 17]. Their near-equality yields a line-like Q-branch in the two-photon spectrum at the band origin (32047.14 cm^{-1}), which corresponds to a laser wavelength of 6,239.08 Å. To the blue and red of the Q-branch are expected very regular (and headless) S- and O-branches, respectively, again because of the near-equality of the rotational constants. The near-symmetry of the $A^2\Pi$–$X^2\Sigma^+$ (4, 0) and $B^2\Sigma^+$–$A^2\Pi$ (3, 4) branch heads with respect to the $B^2\Sigma^+$–$X^2\Sigma^+$ (3, 0) origin, shown in Figure 6, is also due to the similarity in B_v for $B^2\Sigma^+$, $v = 3$ and $X^2\Sigma^+$, $v = 0$. The F_1 and F_2 transitions of the NR2PE O- and S-branches are too closely spaced in energy to be resolved.

Because the OODR transitions are much more easily saturated at high laser intensities than the NR2PE transitions, they may be distinguished by their dependence on laser power. Reduction of the spectral irradiance from $\approx 9 \times 10^{10}$ to $\approx 2 \times 10^6$ W/cm^2 cm^{-1} caused features S, Q, and O to disappear altogether, while neighboring features remained largely unaltered (except for a reduction in line width). Figure 8 shows the effect of this reduction in intensity in the neighborhood of the feature labeled S in Figure 6, which is actually the unresolved S_1 (16) and S_2 (16) lines of the NR2PE. Neighboring S-branch lines that, likewise, disappear at low power are also labeled in Figure 8. Measurements of the fluorescence intensity as a function of irradiance in the range 10^6 – 10^8 W/cm^2 cm^{-1} gave typical power dependencies of ≈ 0.8 for the OODR features and ≈ 1.7 for the NR2PE peaks. Figure 9 shows the fluorescence spectrum observed when the unresolved S (16) lines are pumped by the laser; the upper vibrational level is confirmed to be $v' = 3$.

The probability per unit time for a two-photon transition from a lower state $|g\rangle$ to an upper state $|u\rangle$ is proportional to the quantity

$$\left| \sum_i \frac{\langle u|\mu\cdot E|i\rangle \langle i|\mu\cdot E|l\rangle}{w_{il} - w + i\Gamma_i/2} \right|^2,$$

where μ is the molecular dipole moment, E is the field imposed by the laser, w_{il} is the transition frequency between levels i and l, w is the laser frequency, and Γ_i is the homogeneous width of level i [29–31]. The sum is taken over all intermediate states $|i>$, which may contribute to the two-photon absorption. In the absence of near-resonances, the denominator is effectively a constant for a given two-photon absorption band. Expressions for line strengths in this common case have been derived and vary smoothly with J [30, 31]. However, the detuning of the laser from $A^2\Pi$–$X^2\Sigma^+$ (4, 0) transitions varies from <1 cm^{-1} to ≈400 cm^{-1} as N varies from 0 to 40 for two-photon transitions in $B^2\Sigma^+$–$X^2\Sigma^+$ (3, 0). The corresponding line strengths have been shown to vary over five orders of magnitude [13]. Most significantly, the detuning of the laser from $A^2\Pi$–$X^2\Sigma^+$ (4, 0) transitions that contribute strongly to the two-photon absorption coefficient is the least in each $B^2\Sigma^+$–$X^2\Sigma^+$ (3, 0) $\Delta J = \pm 2$ branch for S_1 (16), S_2 (18), O_1 (18) and O_2 (20). For values of N smaller and larger than these, the detuning increases rapidly [13]. Therefore, these lines and their immediate neighbors are the ones observed in the spectrum (see Figure 8); the others are much weaker and hidden under OODR features. The line-like Q-branch of the two-photon spectrum is strong, not only because it consists of contributions from many transitions, but also because there exist particularly small detunings (<1 cm^{-1}) for several of its transitions. The Q-branch is very easily saturated in spite of the nonresonant nature of its component transitions.

3.5 Unidentified Spectrum: 6,298–6,520 Å. Unidentified features appear in the excitation scan to the red of the $B^2\Sigma^+$–$A^2\Pi$ (3, 4) P_{12} head at 6,298.53 Å, extending to at least 6,520 Å. The entire excitation spectrum observed in this work extending from 6,016–6,520 Å is shown in Appendix B. It should be noted that the spectrum was measured over a number of scans with adjustments to flame conditions and PMT gain between scans. In addition, the spectrum required the use of three dyes (R610/R640, R640, and DCM) and has not been corrected for the variation in laser power over the dye gain curves. The points at which new scans were initiated are indicated in the spectrum. Because of changes in conditions between scans, peak intensities cannot be directly compared over the 500 Å range spanned by the spectrum. The laser was kept focused throughout the entire region. The laser intensity is therefore comparable to that for focused conditions mentioned previously, although no special efforts were made to keep it

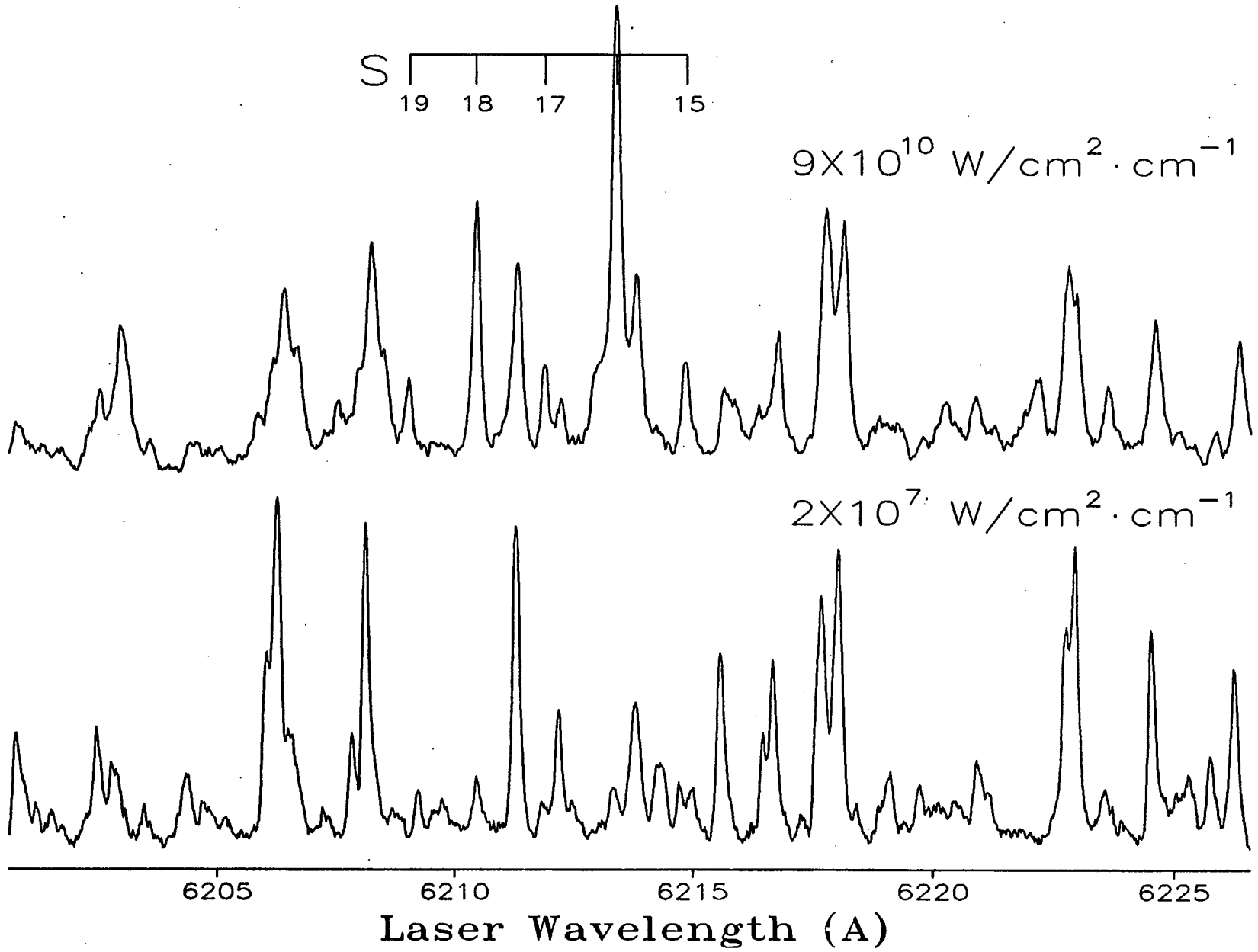

Figure 8. Laser excitation spectra recorded near 6,210 Å at high and low laser irradiance.

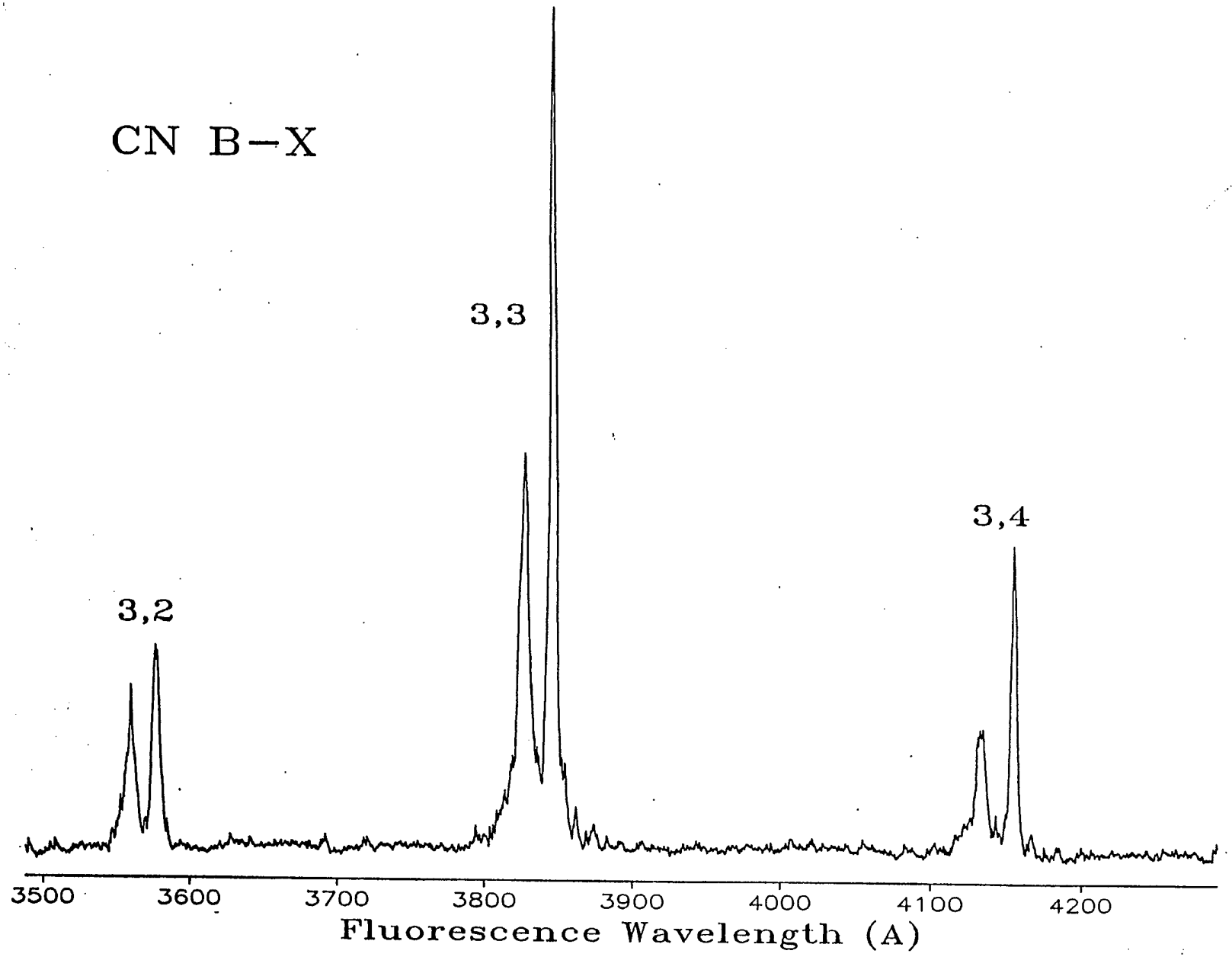

Figure 9. Moderate-resolution LIF spectrum observed while exciting the unresolved S_1 (18) and S_2 (18) transitions in the NR2PE of $B^2\Sigma^+ - X^2\Sigma^+$ (3, 0).

constant between scans. In addition, careful calibration of the laser wavelength was not maintained over the entire range, and the indicated wavelengths must be regarded as only approximate (±2 Å).

With these restrictions in mind, it is nevertheless possible to draw some conclusions regarding the unidentified features to the red of 6,298 Å from the spectrum shown in Appendix B. It must first be noticed that band overlaps between $A^2\Pi - X^2\Sigma^+$ and $B^2\Sigma^+ - A^2\Pi$, which would support another resonant two-photon process, are not present in this wavelength region [19]. It is also clear from a qualitative comparison of the peak heights between scans that the unidentified features are comparable in intensity to those assigned to the $A^2\Pi - X^2\Sigma^+$ (8, 3) and (9, 4) bands in the laser-wavelength range of 6,016–6,180 Å. For these reasons, it is likely that at least some of the features are due to the $A^2\Pi - X^2\Sigma^+$ (10, 5) and (11, 6) bands with R_2 heads at 6,278.9 and 6,432.2 Å, respectively [32], followed by collisional interelectronic conversion to $B^2\Sigma^+$ (v = 0). Recall that a few lines ascribed to the former band that involve perturbed excited-state rotational levels were, in fact, identified near 6,300 Å by using unfocused laser excitation (see section 3.2 and the insert of Figure 6). Branch heads of the former band are hidden in the much stronger OODR region; those of the latter are not readily apparent in the spectrum. It should be noted that while these transitions require pumping out of high-lying vibrational levels of $X^2\Sigma^+$, the term values of the upper levels exceed that of the $B^2\Sigma^+$ (v = 0) level so that an endoergic collision is not required to produce the upper level of the fluorescence transition (Figure 1b).

Another possibility for the source of the unidentified lines is the $B^2\Sigma^+ - A^2\Pi$ $\Delta v = -1$ sequence, specifically the (2, 3) and (1, 2) bands with origins near 6,414 and 6,560 Å, respectively [19]. The spectrum in Appendix B does not extend far enough to the red to identify heads of the latter band, and the former suffers from an extremely unfavorable Franck-Condon factor [19]. Assignment of the unidentified features to either the $A^2\Pi - X^2\Sigma^+$ $\Delta v = 5$ or $B^2\Sigma^+ - A^2\Pi$ $\Delta v = -1$ sequences remains speculative, and the spectrum awaits careful analysis. It should finally be noted that the unidentified features appear to continue to the red of 6,520 Å laser wavelength.

4. SUMMARY

Laser excitation of CN in an atmospheric-pressure CH_4/N_2O flame near 6,000 Å produces the $B^2\Sigma^+$ state by four unique mechanisms. (1) The $B^2\Sigma^+-A^2\Pi$ (0, 0) band is excited in the laser-wavelength range from 5,890 to 6,016 Å. Detection of a molecular excited electronic state in a flame using LIF is comparatively rare. (2) From 6,016 to 6,180 Å the $A^2\Pi-X^2\Sigma^+$ (8, 3) and (9, 4) bands are observed. The $B^2\Sigma^+$ state is populated by collisional interelectronic upconversion from $A^2\Pi$, v = 8, 9. The $A^2\Pi-X^2\Sigma^+$ (8, 3) band overlaps the $B^2\Sigma^+-A^2\Pi$ (0, 0) band and could complicate diagnostic use of the (0, 0) band in collisional environments. The $A^2\Pi-X^2\Sigma^+$ (10, 5) band near 6,300 Å was also observed with significantly enhanced fluorescence following population of $A^2\Pi$, $v' = 10$ levels that are perturbed by $B^2\Sigma^+$, v = 0. (3) From 6,180 to 6,298 Å the overlap of the $A^2\Pi-X^2\Sigma^+$ (4, 0) and $B^2\Sigma^+-A^2\Pi$ (3, 4) bands promotes the detection of a collision-assisted single-color OODR spectrum. The richness of the spectrum is due to rapid rotational relaxation in the $A^2\Pi$, v = 4 level during the laser pulse. (4) Overlying the OODR features are peaks due to NR2PE of CN in the $B^2\Sigma^+-X^2\Sigma^+$ (3, 0) band with $A^2\Pi$, v = 4 providing the near-resonant energy levels. The only NR2PE transitions observed are those for which the laser is detuned from a resonance in $A^2\Pi-X^2\Sigma^+$ (4, 0) by less than 20 cm^{-1}.

In addition to observation of the spectra assigned to the four processes in the region from 5,890–6,298 Å, a rich specctrum was observed from 6,298–6,520 Å. The latter region awaits analysis. The spectrum is given in Appendix B. It appears likely the spectrum continues to longer wavelengths.

This work has shown that the CH_4/N_2O flame may be used as a relatively simple and inexpensive source of CN $A^2\Pi$ as well as $X^2\Sigma^+$ for study by any number of spectroscopic techniques. However, use of LIF in this environment can be complicated by unexpected collisional and two-photon absorption processes. Employment of LIF as a quantitative diagnostic in such environments requires the recognition of possible interferences due to these mechanisms. This work has identified the gross mechanistic features giving rise to the observed spectra; it will hopefully inspire future efforts to quantify the unique effects involved in their production.

5. REFERENCES

1. Huber, K. P., and G. Herzberg. Molecular Spectra and Molecular Structure, vol. 4, Constants of diatomic molecules. New York: Van Nostrand Reinhold, pp. 154–157, 1979.

2. LeBlanc, F. J. "$B^2\Sigma \rightarrow A^2\Pi_i$ Bands of CN." Journal of Chemical Physics, vol. 48, p. 1841, 1968.

3. Halpern, J. B., and X. Tang. "Production of CN ($A^2\Pi_i$) in the Photolysis of Acetonitrile at 158 nm." Chemical Physics Letters, vol. 122, p. 294, 1985.

4. Furio, N., A. Ali, and P. J. Dagdigian. "Laser Excitation of the Overlapping CN B-A (8, 7) and B-X (8, 11) Bands: The Relative Phase of the B-A and B-X Transition Moments." Journal of Molecular Spectroscopy, vol. 134, p. 199, 1989.

5. Ali, A. A., G. Jihua, and P. J. Dagdigian. "State-Resolved Inelastic Cross Sections From CN $A^2\Pi$ v = 8 to $X^2\Sigma^+$ v = 12: Quenching of the Even-Odd Alternation in the Final Rotational State Populations." Journal of Chemical Physics, vol. 87, p. 2045, 1987.

6. Furio, N., A. Ali, and P. J. Dagdigian. "State-Resolved Study of Collisional Energy Transfer Between $A^2\Pi$ v = 7 and $X^2\Sigma^+$ v = 11 Rotational Levels of CN." Journal of Chemical Physics, vol. 85, p. 3860, 1986.

7. Furio, N., A. Ali, and P. J. Dagdigian. "Interference Effects in Rotational-State-Resolved Collisional Energy Transfer Between the $A^2\Pi$ and $B^2\Sigma^+$ States of CN." Chemical Physics Letters, vol. 125, p. 561, 1986.

8. Pinchemel, B., and P. J. Dagdigian. "Collisional Vibrational Relaxation in the $A^2\Pi$ State of CN." Chemical Physics Letters, vol. 106, p. 313, 1984.

9. Jihua, G., A. Ali, and P. J. Dagdigian. "State-to-State Collisional Interelectronic and Intraelectronic Energy Transfer Involving CN $A^2\Pi$ v = 3 and $X^2\Sigma^+$ v = 7 Rotational Levels." Journal of Chemical Physics, vol. 85, p. 7098, 1986.

10. Conley, C., J. B. Halpern, J. Wood, C. Vaughn, and W. M. Jackson. "Laser Excitation of the CN $B^2\Sigma^+ \leftarrow A^2\Pi$ 0-0 and 1-0 bands." Chemical Physics Letters, vol. 73, p. 224, 1980.

11. Halpern, J. B., and X. Tang. "Oscillator Strength of the CN $A^2\Pi_i \rightarrow B^2\Sigma^+$ (0, 0) Transition." Chemical Physics Letters, vol. 97, p. 170, 1983.

12. Vanderhoff, J. A., R. A. Beyer, A. J. Kotlar, and W. R. Anderson. "Kr^+ and Ar^+ Laser-Excited Fluorescence of CN in a Flame." Applied Optics, vol. 22, p. 1976, 1983.

13. Guthrie, J. A., W. R. Anderson, A. J. Kotlar, Y. Haung, and J. B. Halpern. "Strong Resonance Enhancement of the CN Two-Photon Absorption $B^2\Sigma^+ \leftarrow X^2\Sigma^+$ (3, 0) by the $A^2\Pi_i$, v′ = 4 Level." Journal of Chemical Physics, vol. 100, p. 8713, 1994.

14. Beyer, R. A., and M. A. DeWilde. "Simple Burner for Laser Probing of Flames." Reviews of Scientific Instruments, vol. 53, p. 103, 1982.

15. Vanderhoff, J. A., R. A. Beyer, A. J. Kotlar, and W. R. Anderson. Ar^+ Laser-Excited Fluorescence of C_2 and CN Produced in a Flame." Combustion and Flame, vol. 49, p. 197, 1983.

16. Kotlar, A. J., R. W. Field, J. I. Steinfield, and J. A. Coxon. "Analysis of Perturbations in the $A^2\Pi$-$X^2\Sigma^+$ "Red" System of CN." Journal of Molecular Spectroscopy, vol. 80, p. 86, 1980.

17. Engleman, R. "The $\Delta v = 0$ and +1 Sequence Bands of the CN Violet System Observed During the Flash Photolysis of BrCN." Journal of Molecular Spectroscopy, vol. 49, p. 106, 1974.

18. Costes, M., C. Naulin, and G. Dorthe. "Einstein Coefficient of the CN $B^2\Sigma^+$-$A^2\Pi_i$ (0, 0) Band." Chemical Physics Letters, vol. 113, p. 569, 1985.

19. Knowles, P. J., H. Werner, P. J. Hay, and D. C. Cartwright. "The $A^2\Pi$-$X^2\Sigma^+$ Red and $B^2\Sigma$-$X^2\Sigma^+$ Violet Systems of the CN Radical: Accurate Multireference Configuration Interaction Calculations of the Radiative Transition Probabilities." Journal of Chemical Physics, vol. 89, p. 7334, 1988.

20. Ali, A., J. Guo, and P. J. Dagdigian. "Collisionless and Collision-Induced B-X Emission From Laser-Excited CN $A^2\Pi$ v = 10 Rotational Levels." Chemical Physics Letters, vol. 131, p. 331, 1986.

21. Kiess, N. H., and H. P. Broida. "Perturbations and Rotational Intensities Observed in CN Bands Emitted by Reactions of Organic Molecules With Nitrogen Atoms." Journal of Molecular Spectroscopy, vol. 7, p. 194, 1961.

22. Katayama, D. H., T. A. Miller, and V. E. Bondybey. "Radiative Decay and Radiationless Deactivation in Selectively Excited CN." Journal of Chemical Physics, vol. 71, p. 1662, 1979.

23. Crosley, D. R. "Collisional Effects on Laser-Induced Fluorescence Flame Measurements." Optical Engineering, vol. 20, p. 511, 1981.

24. Crosley, D. R., and G. P. Smith. "Laser-Induced Fluorescence Spectroscopy for Combustion Diagnostics." Optical Engineering, vol. 22, p. 545, 1983.

25. Stepowski, D., and M. J. Cottereau. "Time Resolved Study of Rotational Energy Transfer in $A^2\Sigma^+$ ($v' = 0$) State of OH in a Flame by Laser Induced Fluorescence. Journal of Chemical Physics, vol. 74, p. 6674, 1981.

26. Anderson, W. R., K. N. Wong, and A. J. Kotlar. U.S. Army Research Laboratory, Aberdeen Proving Ground, MD, to be published.

27. Balz, J. G., R. A. Bernheim, L. P. Gold, P. B. Kelly, and D. K. Veirs. "The Optical-Optical Double Resonance Spectrum of $^7Li_2$ Produced by a Single Tunable CW Laser." Journal of Chemical Physics, vol. 75, p. 5226, 1981.

28. Balz, J. G., R. A. Bernheim, and L. P. Gold. "Optical-Optical Double Resonance and Double Resonance Multiphoton Ionization in $^7Li_2$ Produced by Single CW Dye Laser Excitation." Journal of Chemical Physics, vol. 86, p. 1, 1986.

29. Bebb, H. B., and A. Gold. "Multiphoton Ionization of Hydrogen and Rare Gase Atoms." Physical Review, vol. 143, p. 1, 1966.

30. Bray, R. G., and R. M. Hochstrasser. "Two-Photon Absorption by Rotating Diatomic Molecules." Molecular Physics, vol. 31, p. 1199, 1976.

31. Halpern, J. B., H. Zacharias, and R. Wallenstein. "Rotational Line Strengths in Two- and Three-Photon Transitions in Diatomic Molecules." Journal of Molecular Spectroscopy, vol. 79, p. 1, 1980.

32. Pearse, R. W. B., and A. G. Gaydon. The Identification of Molecular Spectra. John Wiley and Sons, NY, 1976.

INTENTIONALLY LEFT BLANK.

APPENDIX A:

$B^2\Sigma^+ - A^2\Pi$ (0, 0) BAND EXCITATION SPECTRUM FROM 5,890 TO 6,016 Å

INTENTIONALLY LEFT BLANK.

This appendix contains the $B^2\Sigma^+ - A^2\Pi$ (0, 0) band excitation spectrum from 5,890 to 6,016 Å (extended further to the blue than in Figure 3). The spectrum has not been normalized with respect to laser power. The spectrum is composed of two separate scans. The point at which the second scan was initiated is indicated near 5,970 Å. The scan on consecutive pages is continuous except when "new scan" appears. Neglecting the variation in laser power over both scans, peak intensities may be directly compared since operating conditions were identical for both scans.

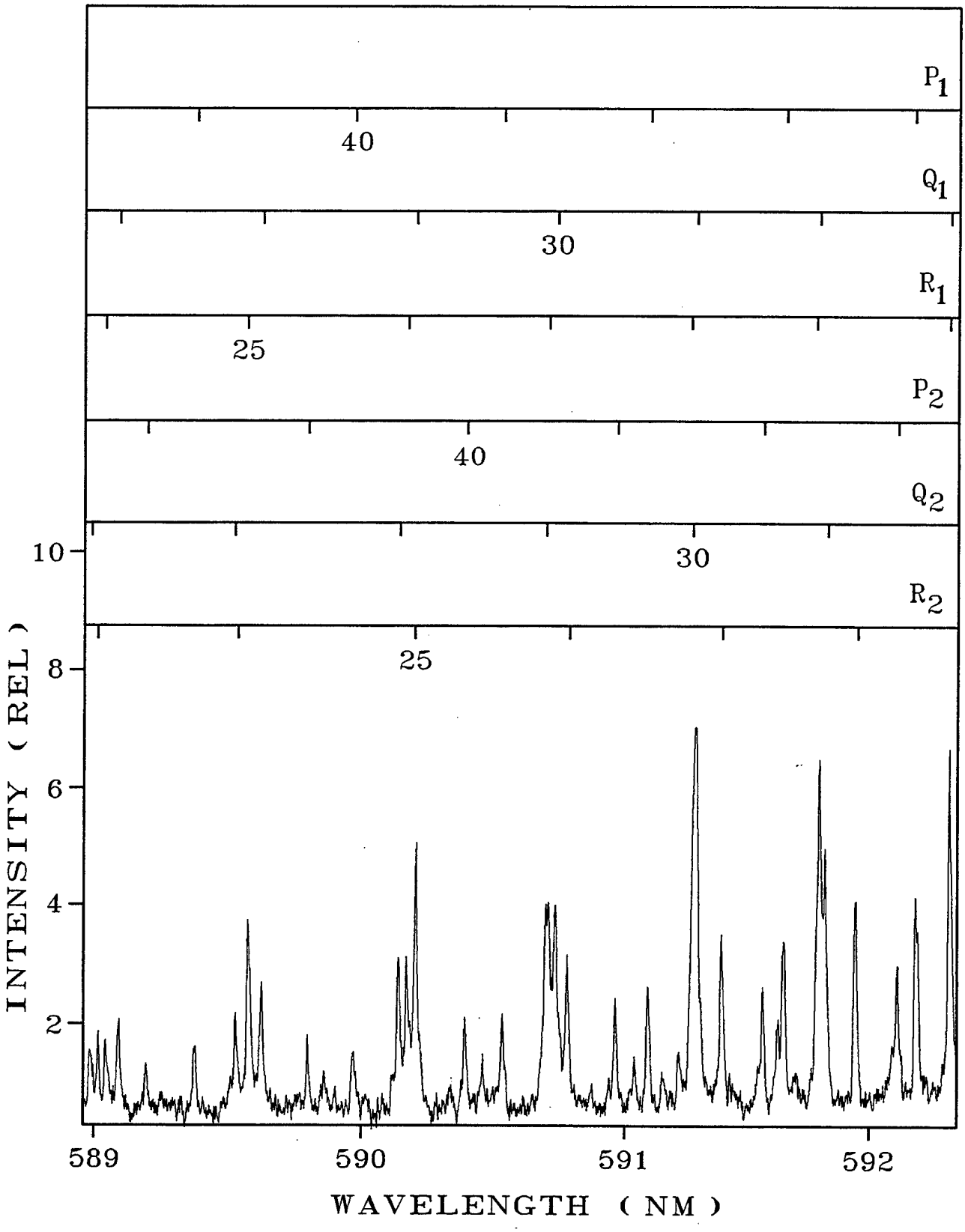

Figure A-1. The CN $B^2\Sigma^+$–$A^2\Pi$ (0, 0) band excitation spectrum from 5,890 to 6,016 Å.

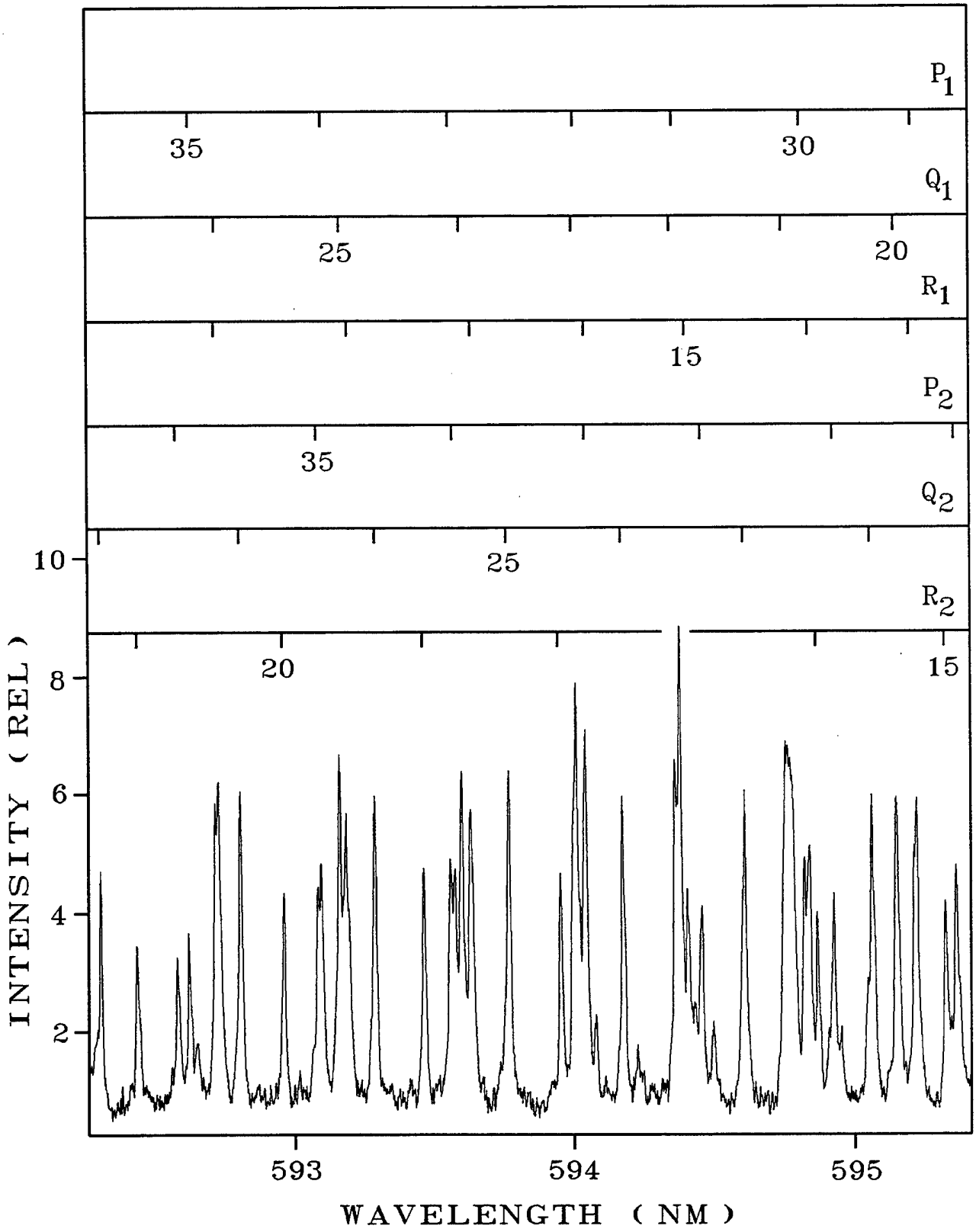

Figure A-1. (Continued).

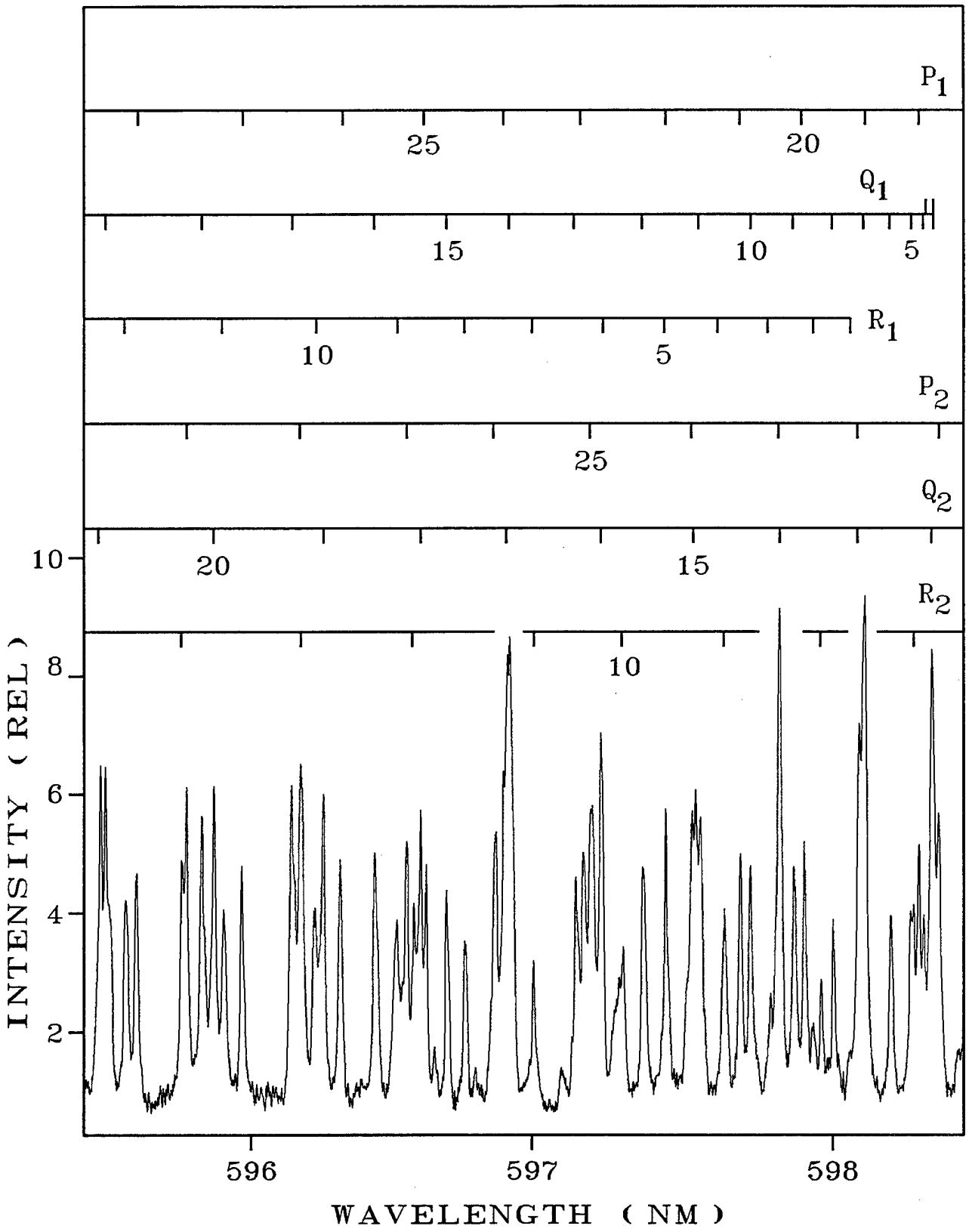

Figure A-1. (Continued).

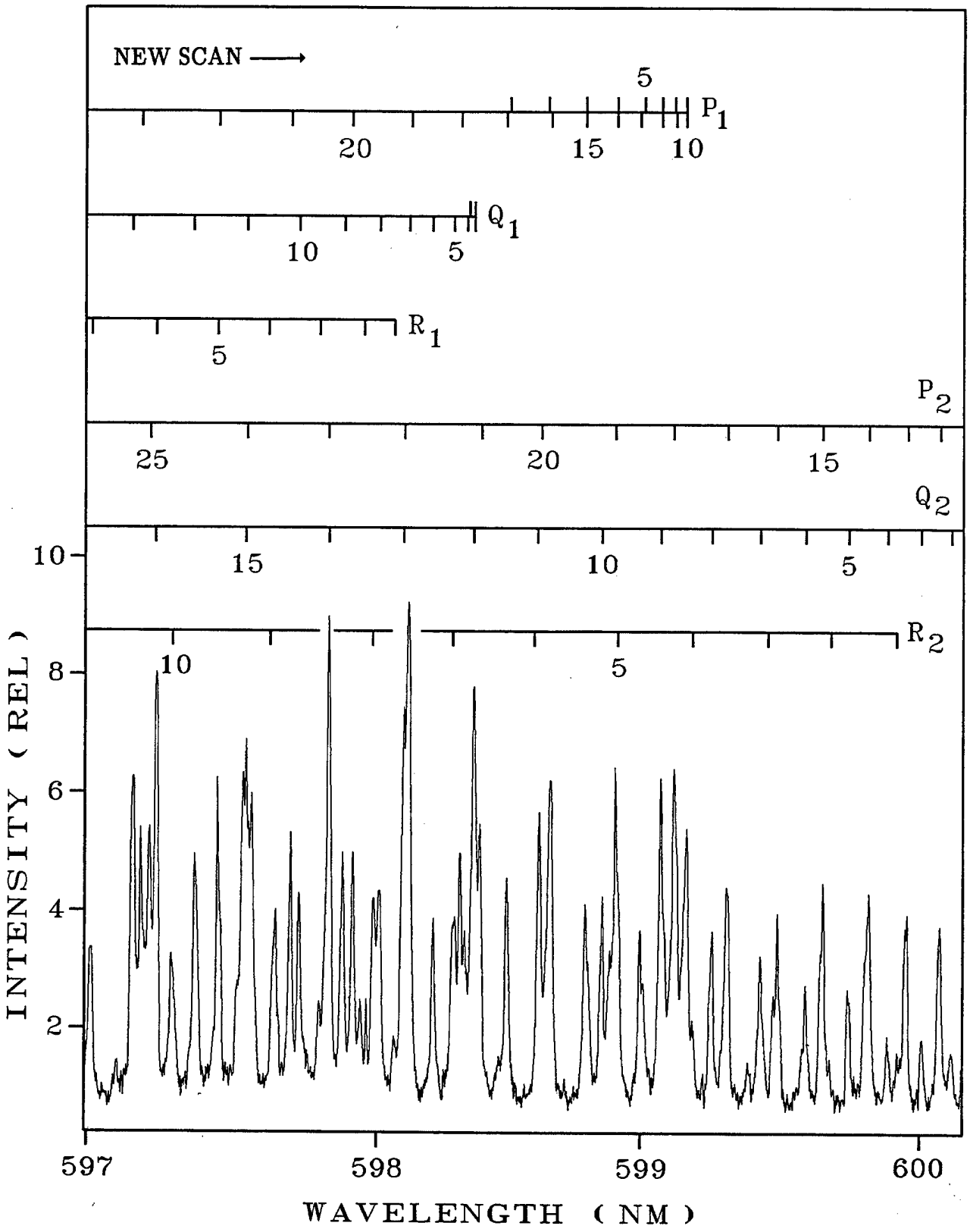

Figure A-1. (Continued).

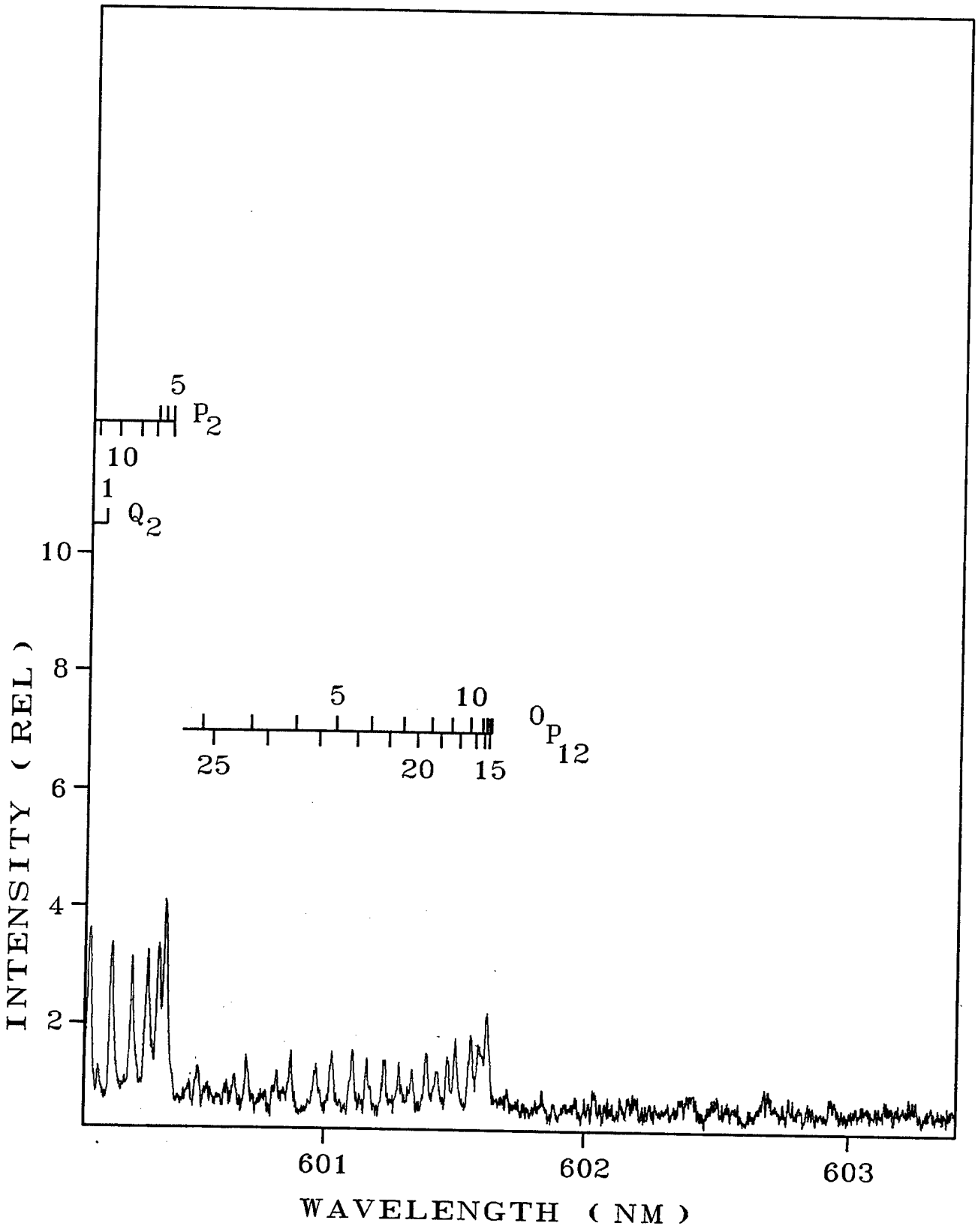

Figure A-1. (Continued).

APPENDIX B:

CN EXCITATION SPECTRUM FROM 6,016 TO 6,520 Å

INTENTIONALLY LEFT BLANK.

This appendix contains the excitation spectrum observed from 6,016 to 6,520 Å by detecting fluorescence near 3,860 Å. All of the scans were taken with the laser beam focused. The scans on consecutive pages are continuous except where "new scan" appears. Because of changing conditions between scans and variations in laser power over three dye gain curves, comparisons of peak intensities must be made cautiously. At the time these spectra were taken, the dye laser-wavelength drive was malfunctioning, resulting in nonlinear scan rates. The etalon fringe pattern is therefore superimposed on the spectrum from 6,016 to 6,520 Å to aid in rough calibration of the wavelength scale. In this wavelength region, fringes are separated by ~1.6 Å. The assigned wavelengths are accurate only to within about ±2 Å, but fringe locations over short wavelength ranges should yield an accurate relative wavelength calibration. Regions in which a "flame adjustment" is indicated must be discarded; there are few of these, and they are short. In these regions, the laser-wavelength was scanning. However, some change in flame conditions (e.g., blowout) required operator attention to correct and optimize signal.

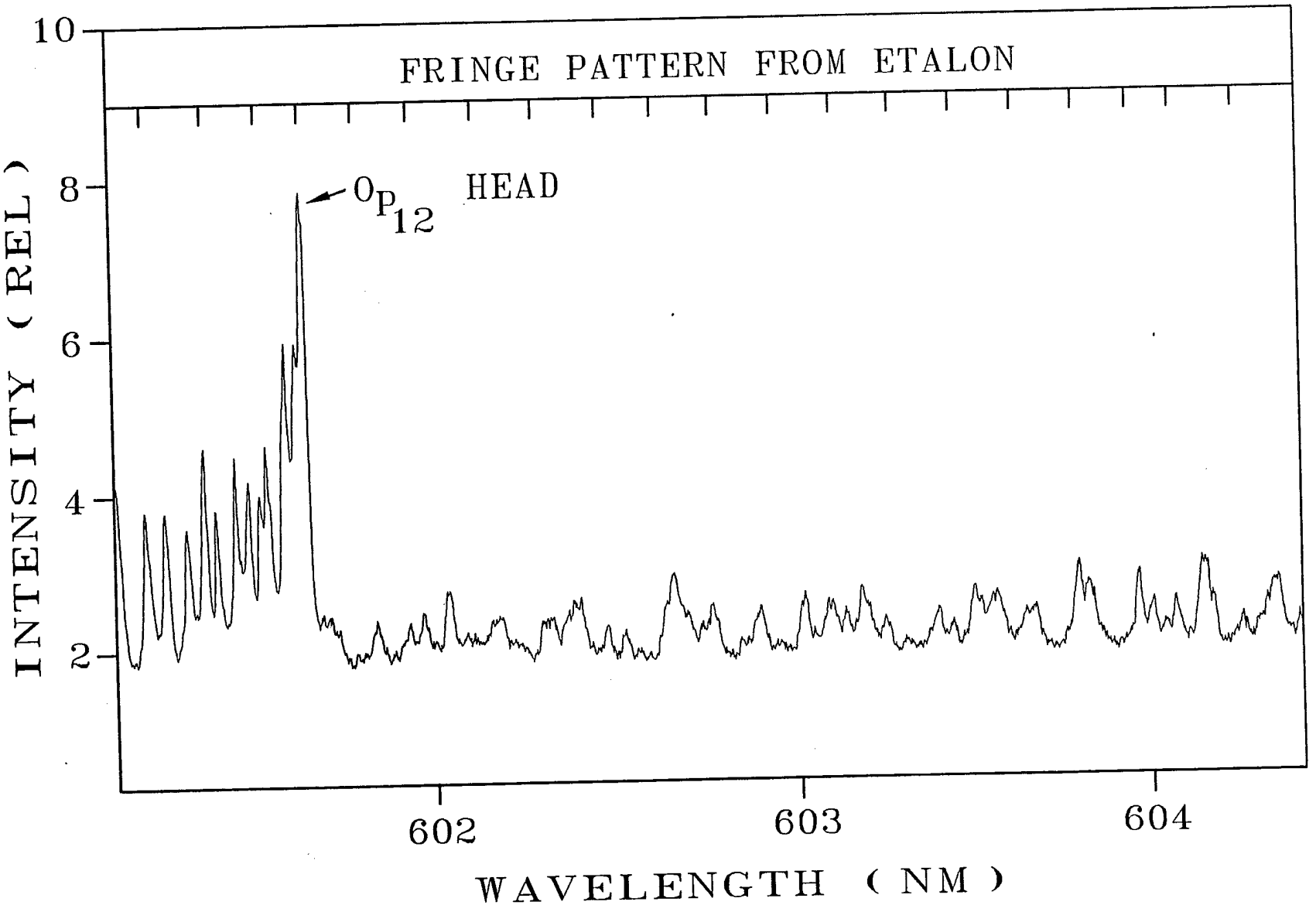

Figure B-1. The CN $B^2\Sigma^+$ excitation spectrum observed from 6,016 to 6,520 Å.

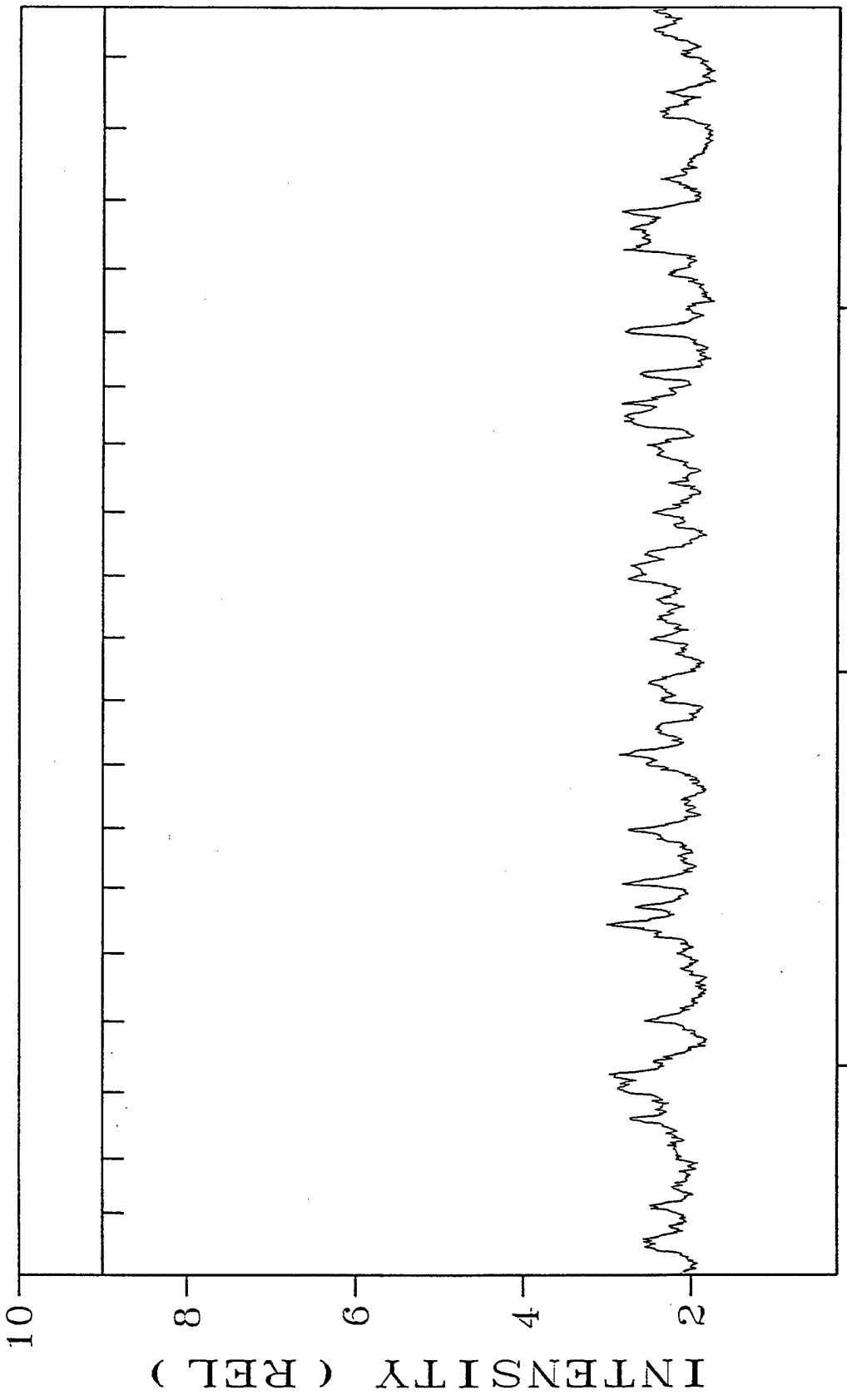

Figure B-1. (Continued).

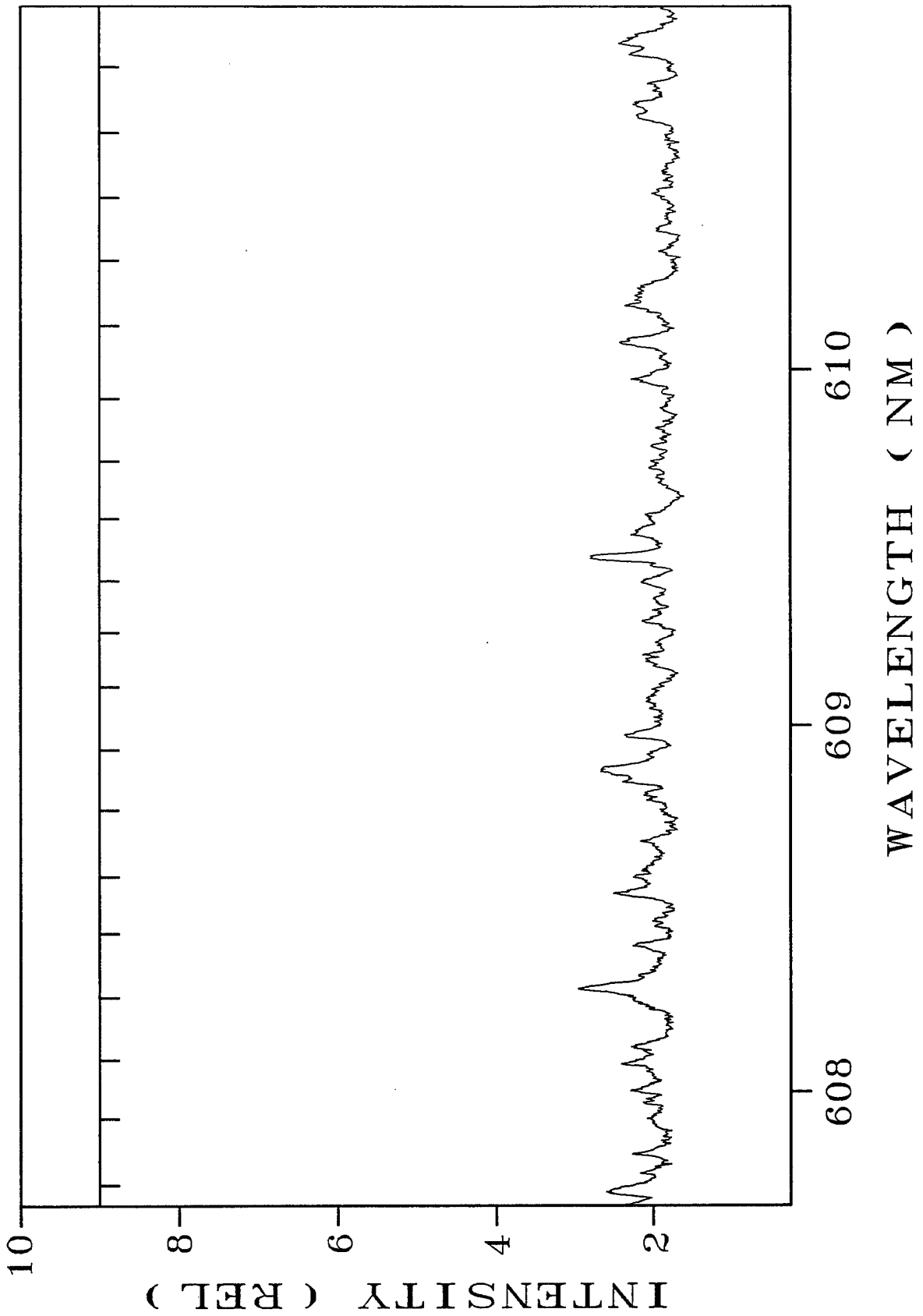

Figure B-1. (Continued).

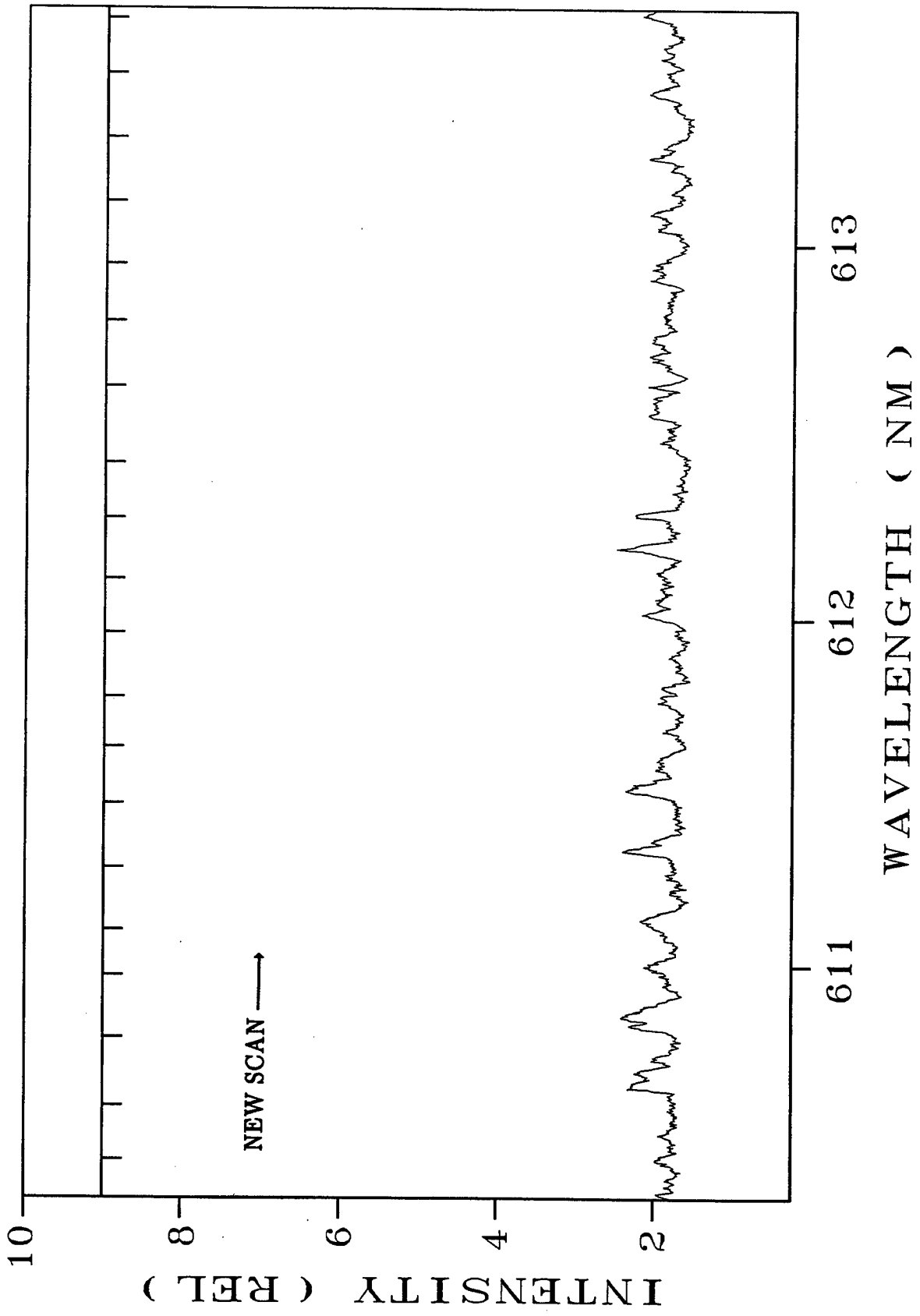

Figure B-1. (Continued).

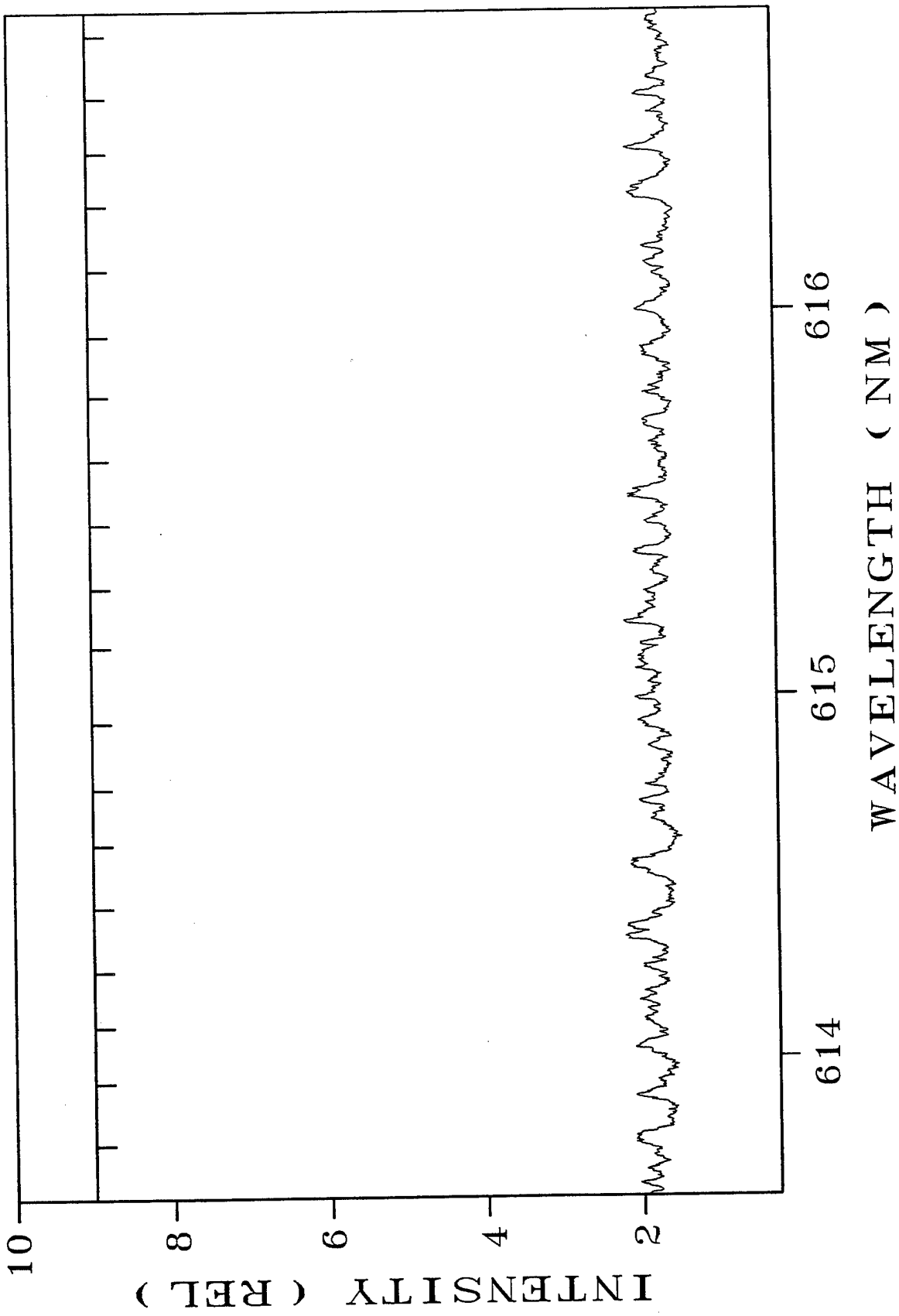

Figure B-1. (Continued).

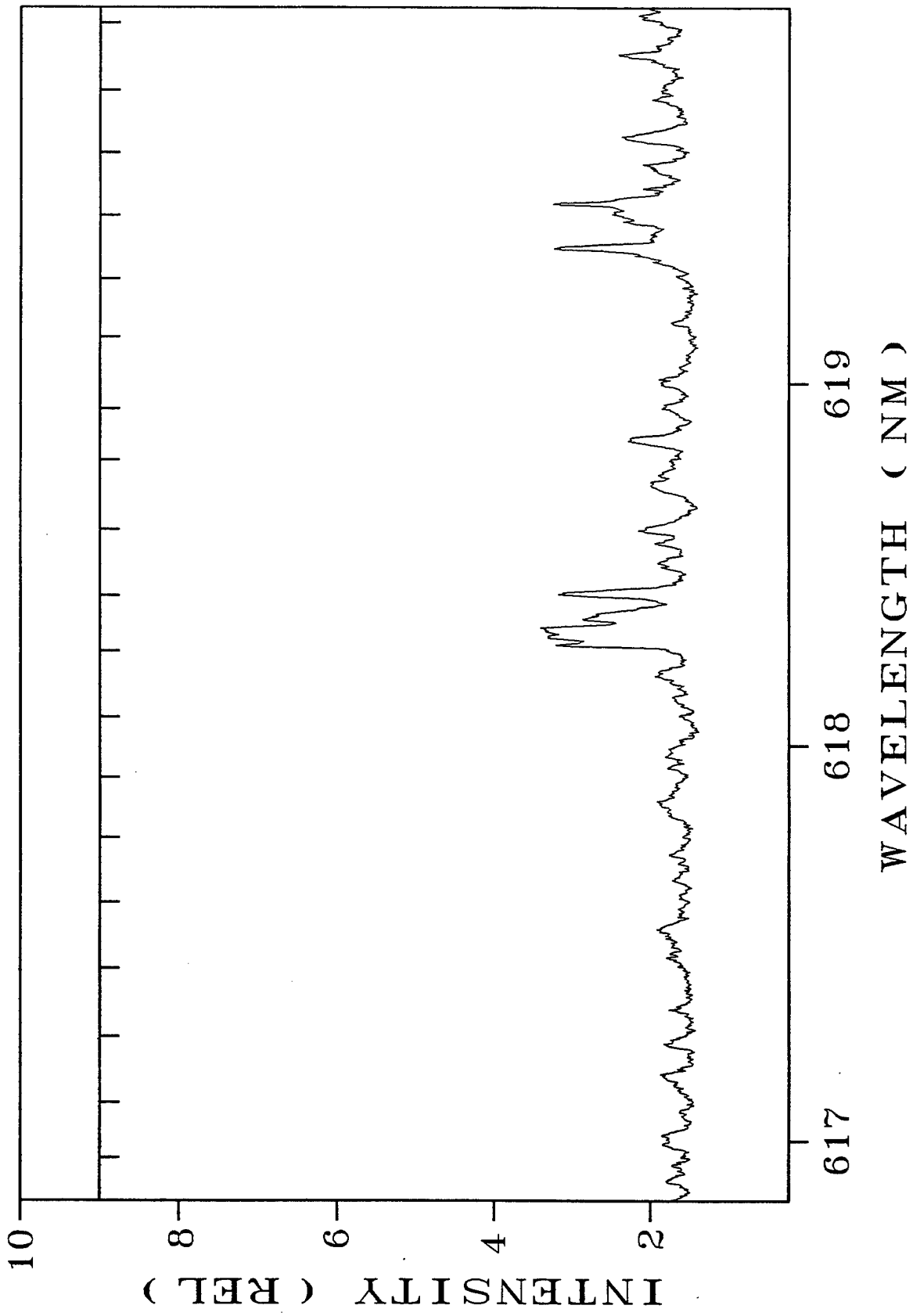

Figure B-1. (Continued).

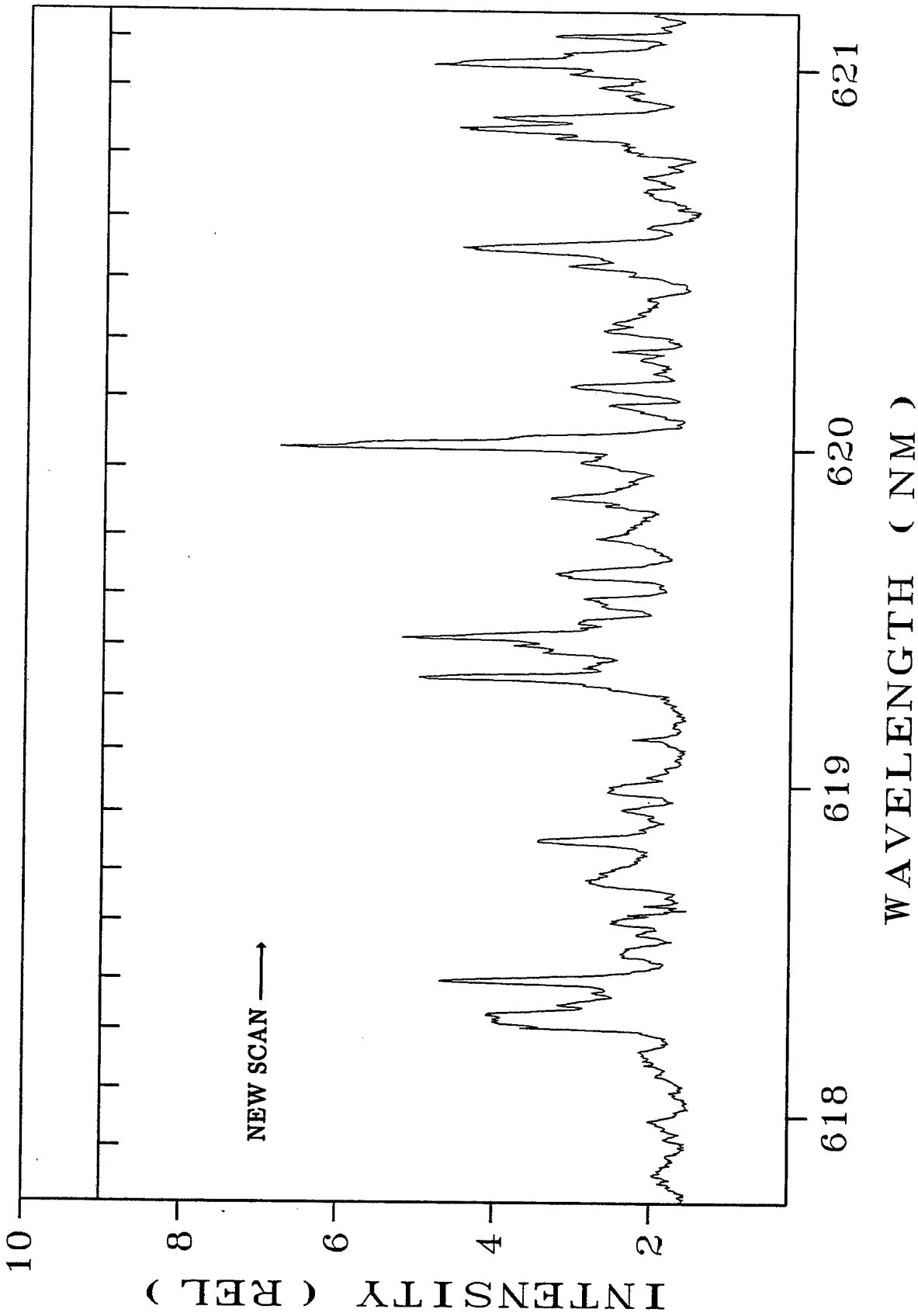

Figure B-1. (Continued).

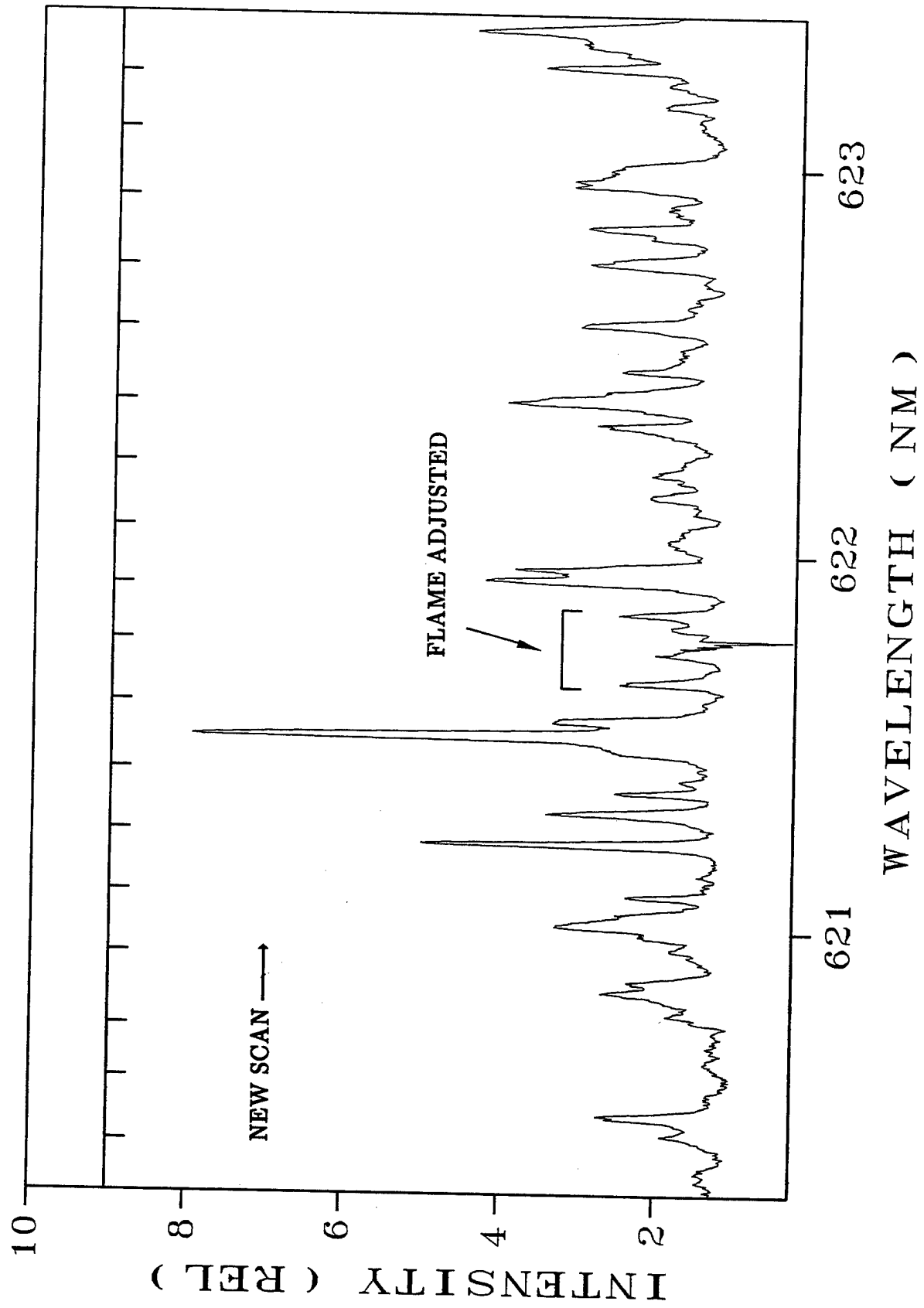

Figure B-1. (Continued).

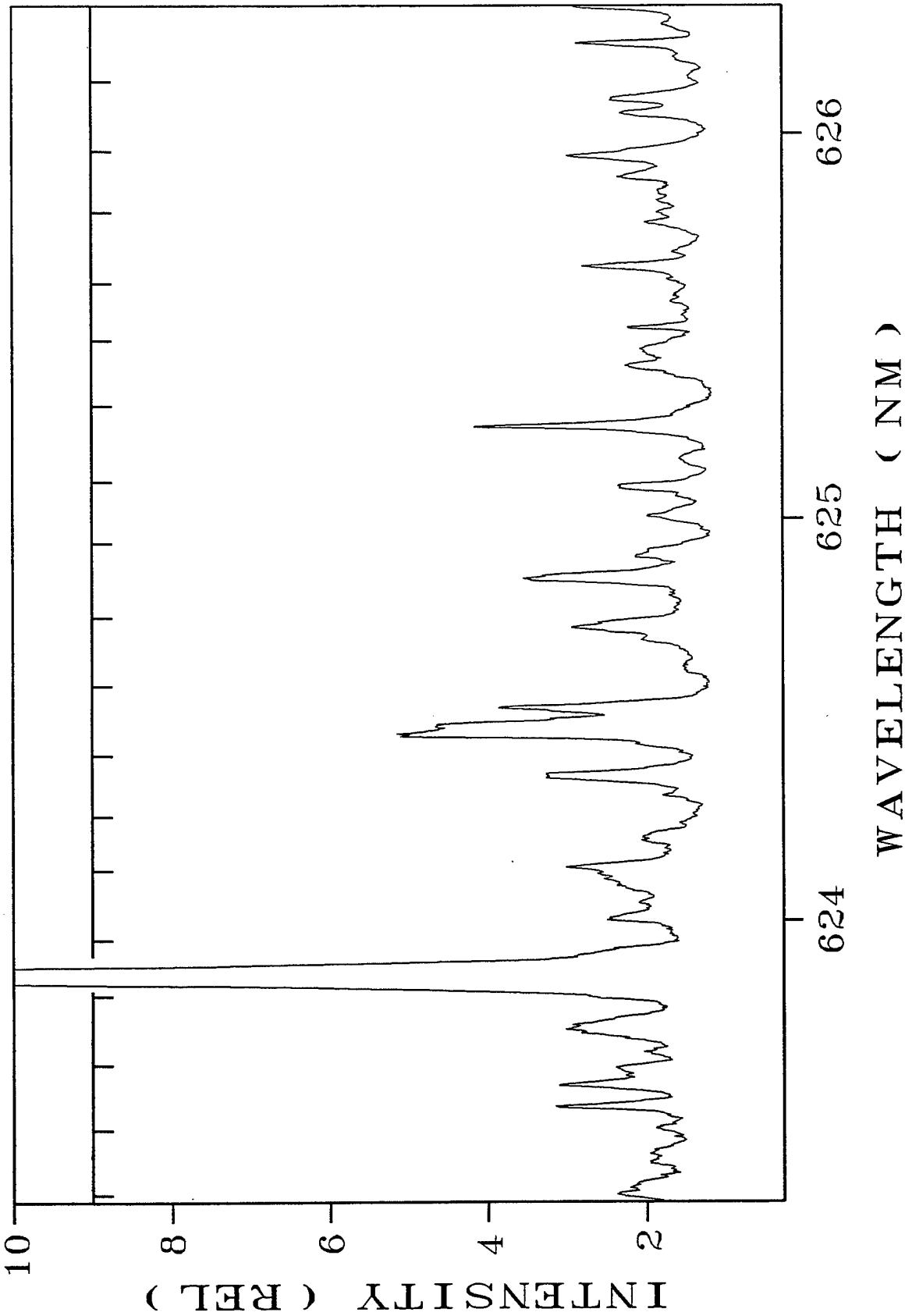

Figure B-1. (Continued).

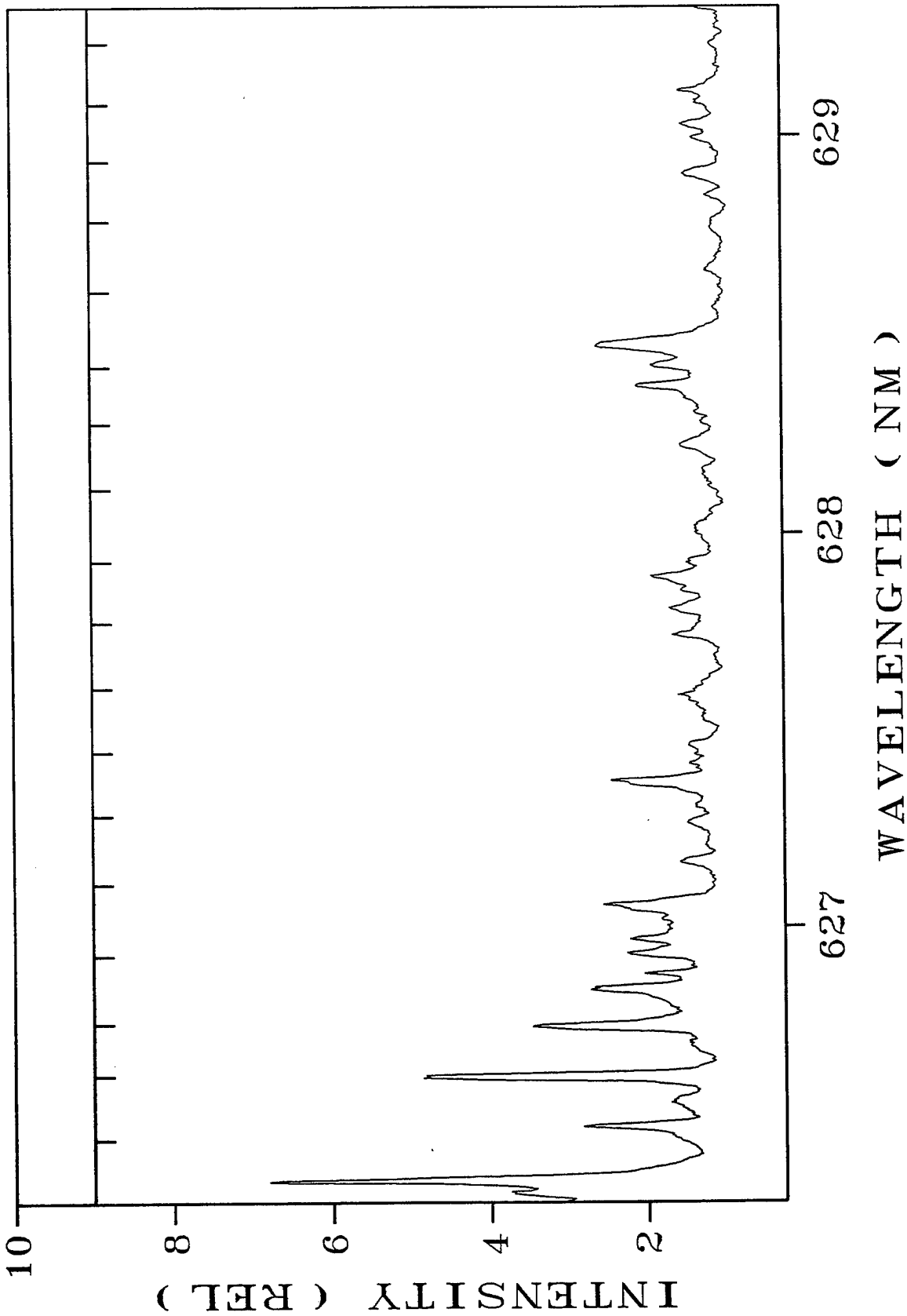

Figure B-1. (Continued).

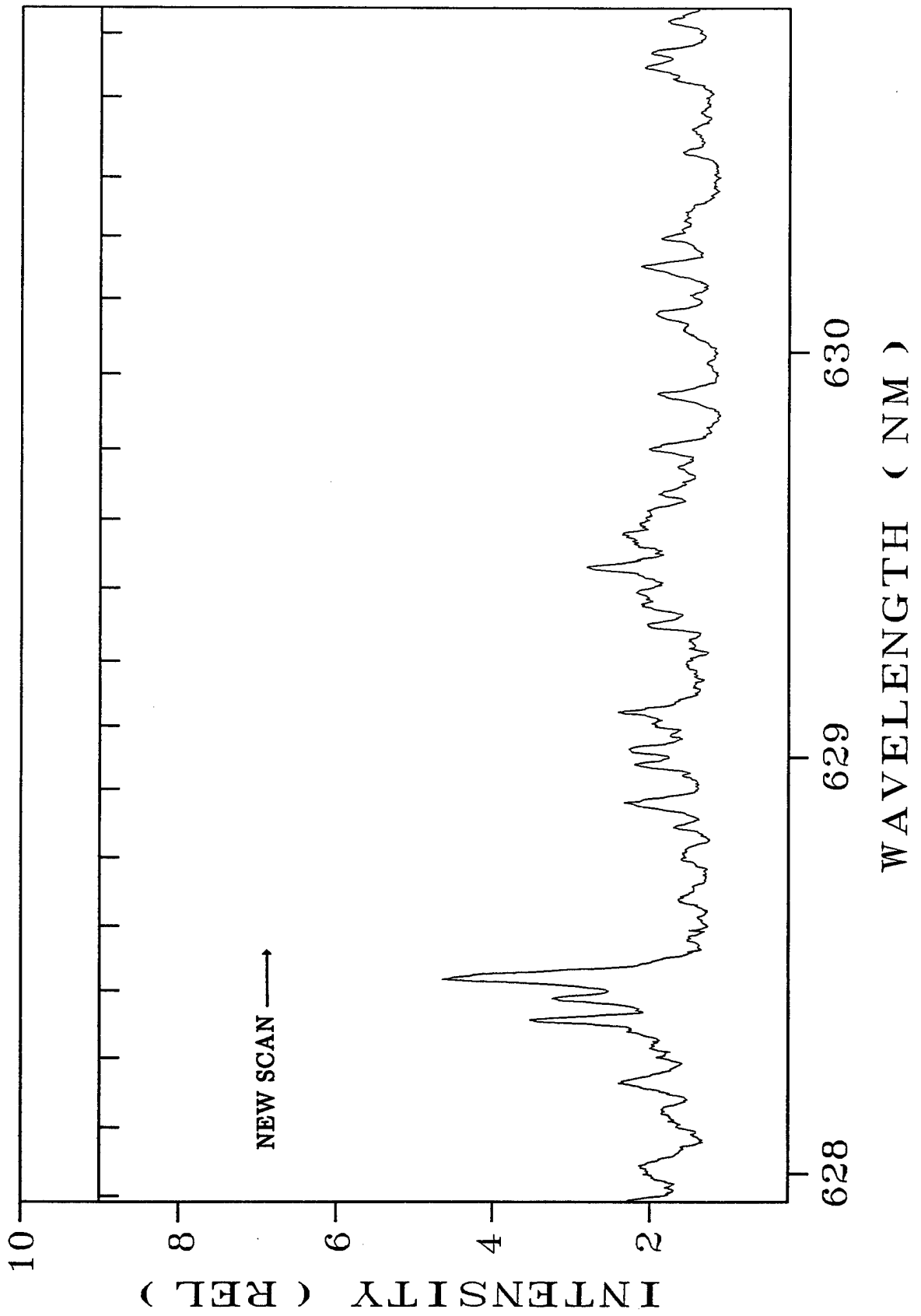

Figure B-1. (Continued).

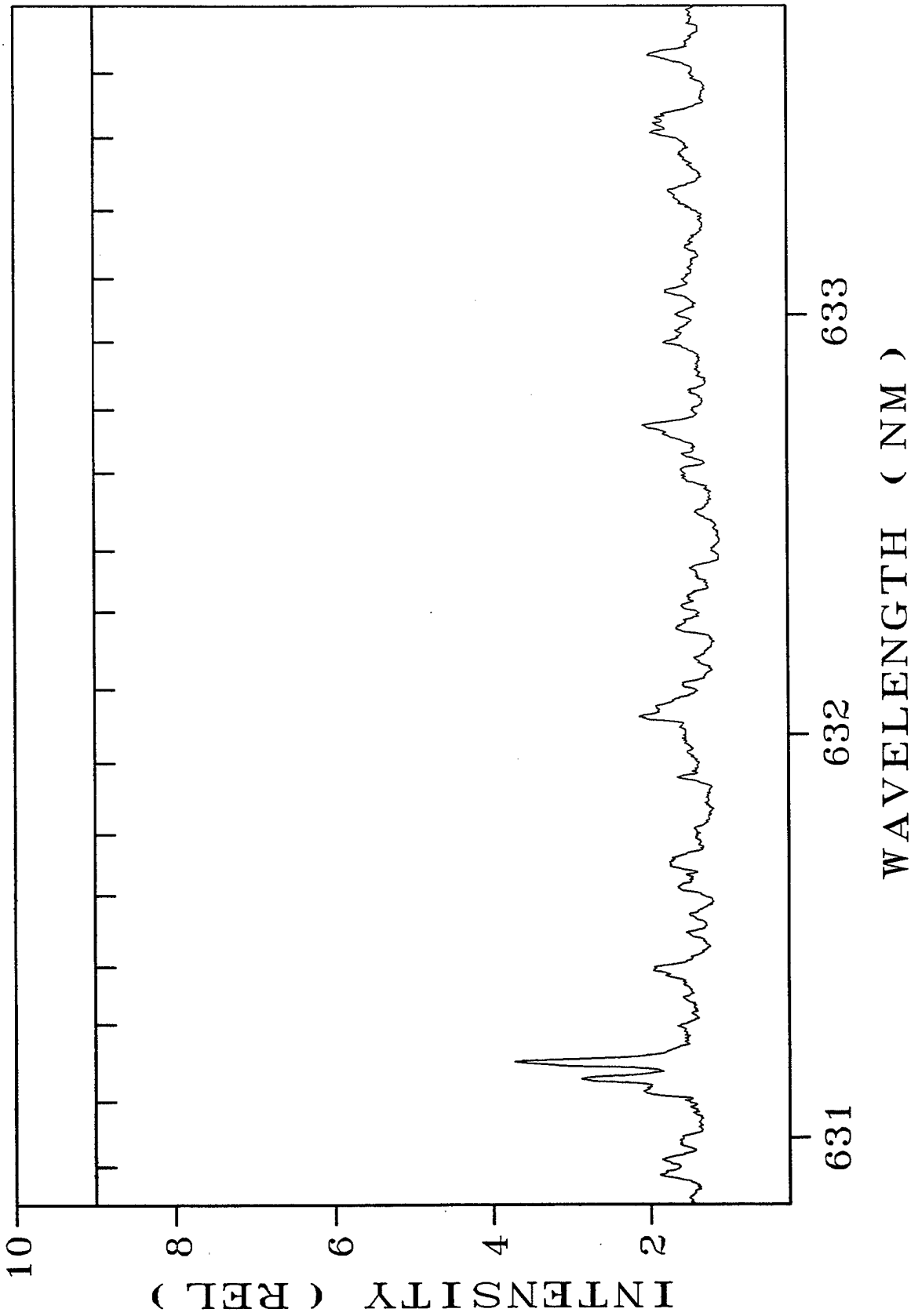

Figure B-1. (Continued).

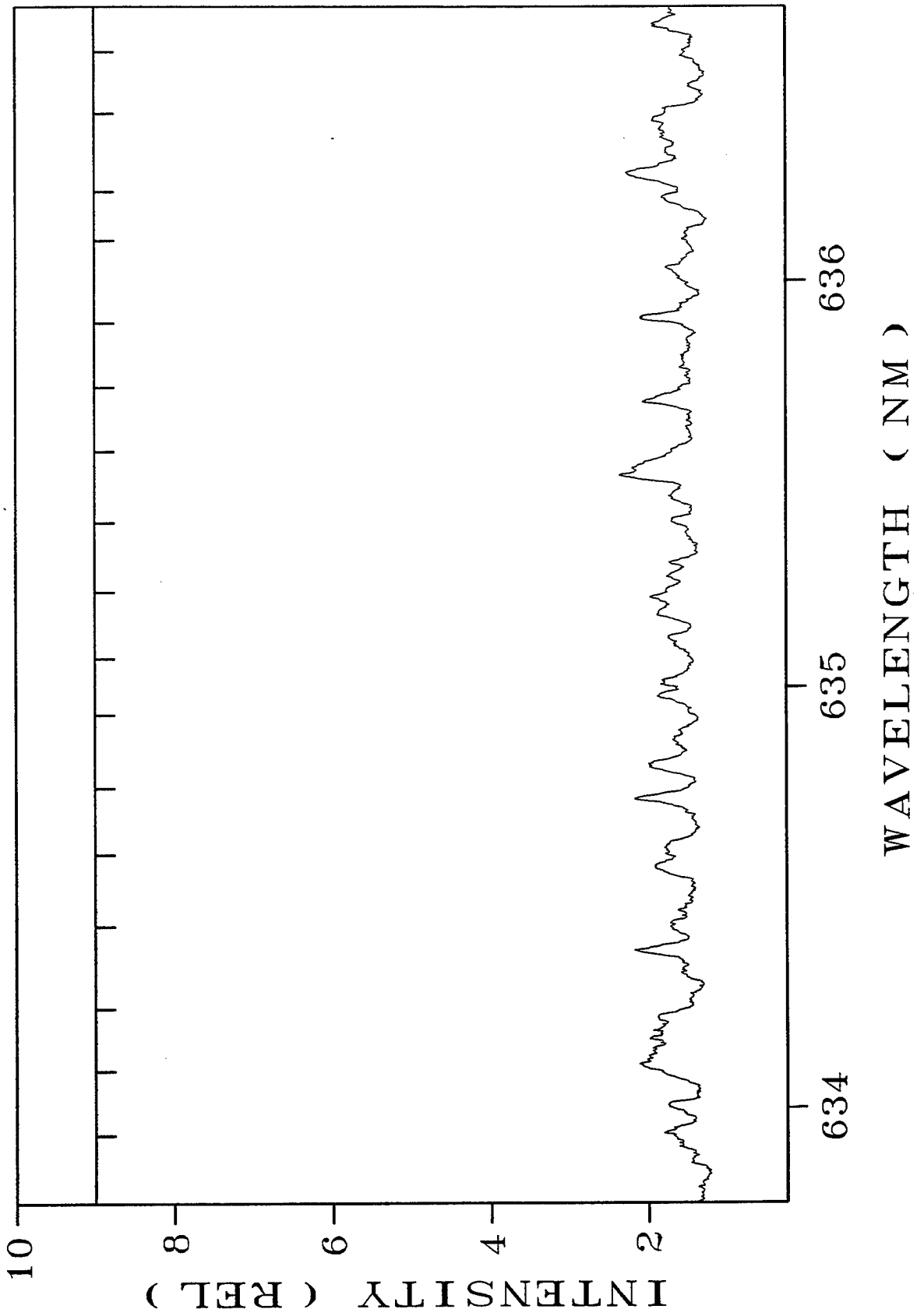

Figure B-1. (Continued).

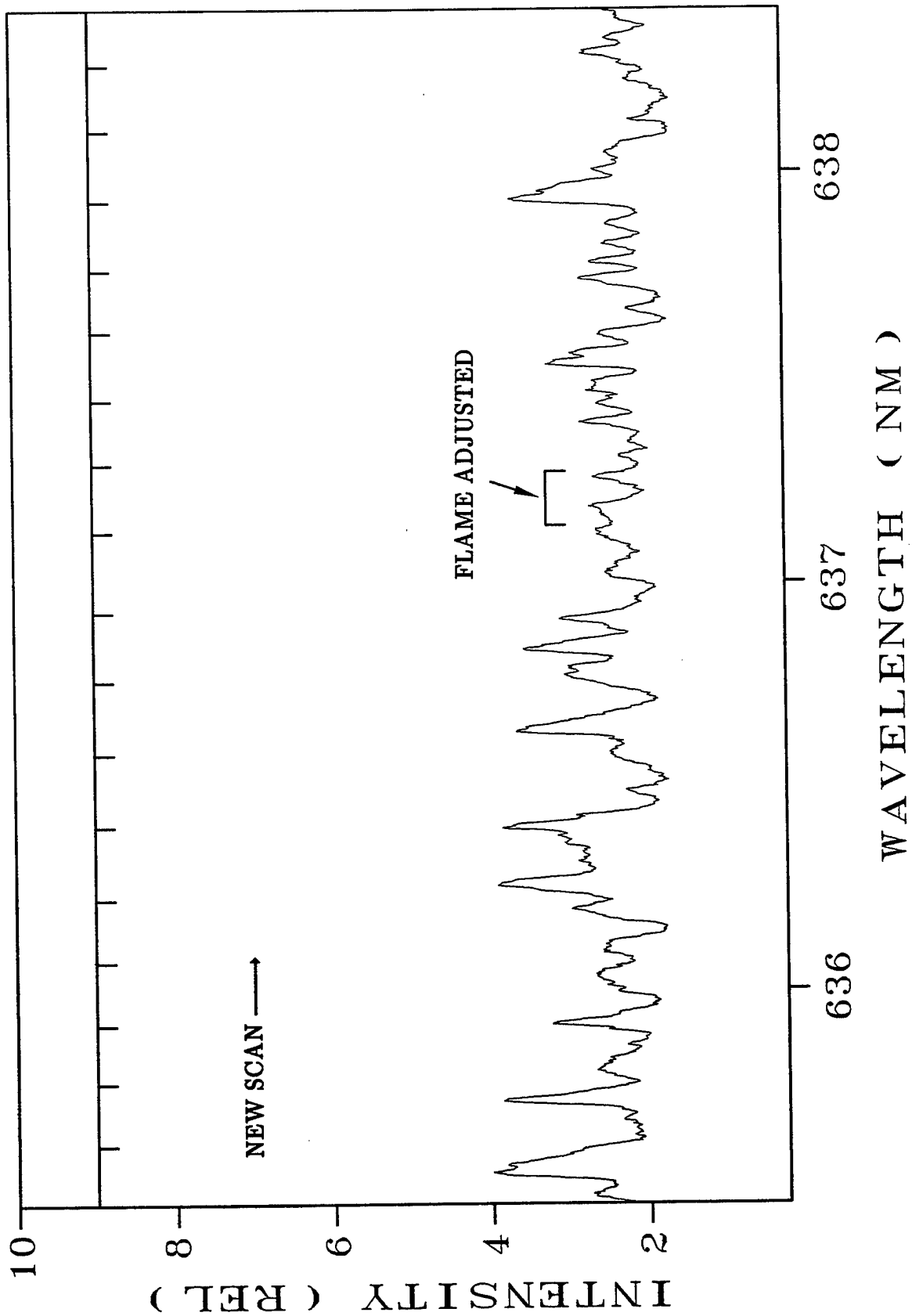

Figure B-1. (Continued).

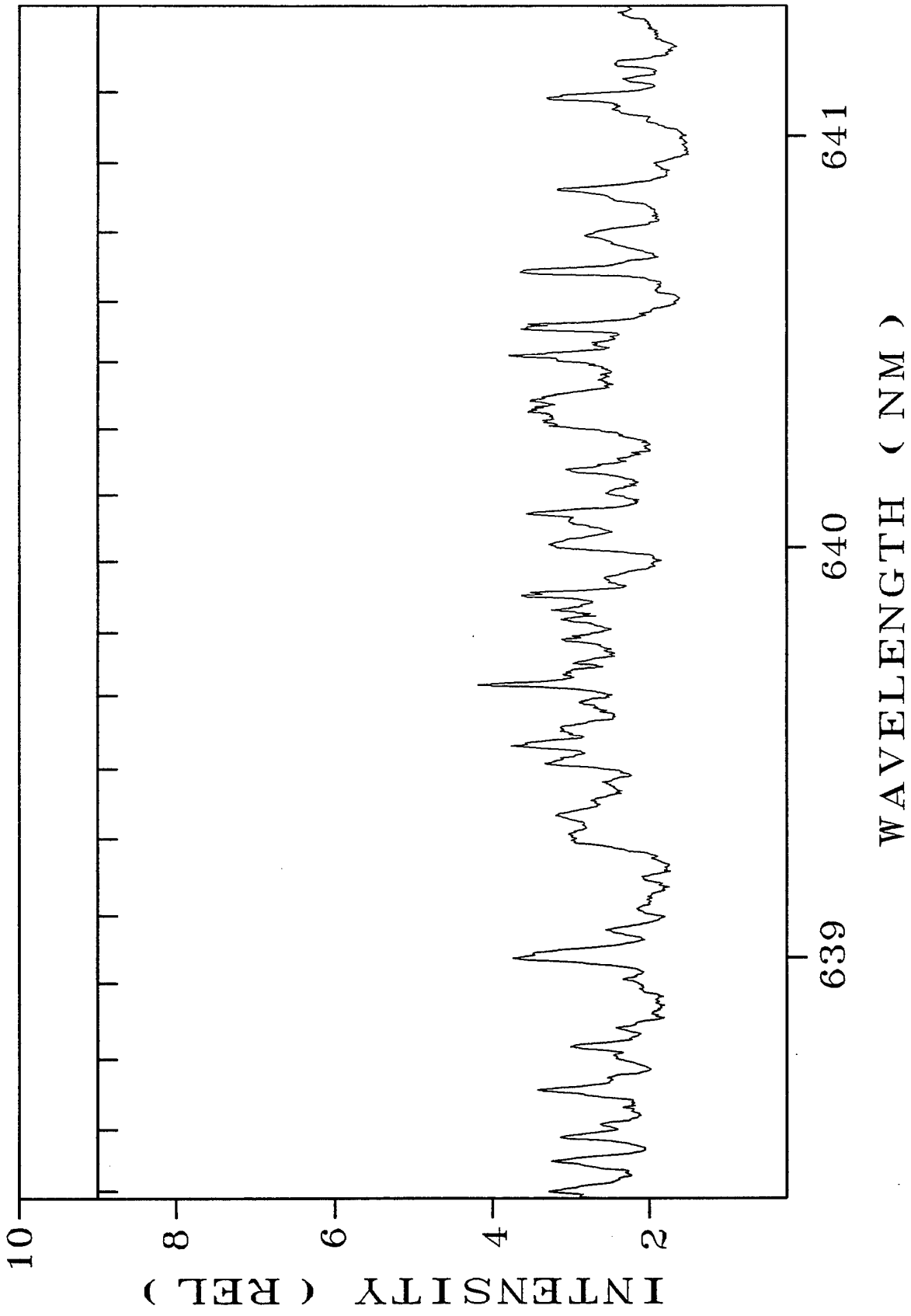

Figure B-1. (Continued).

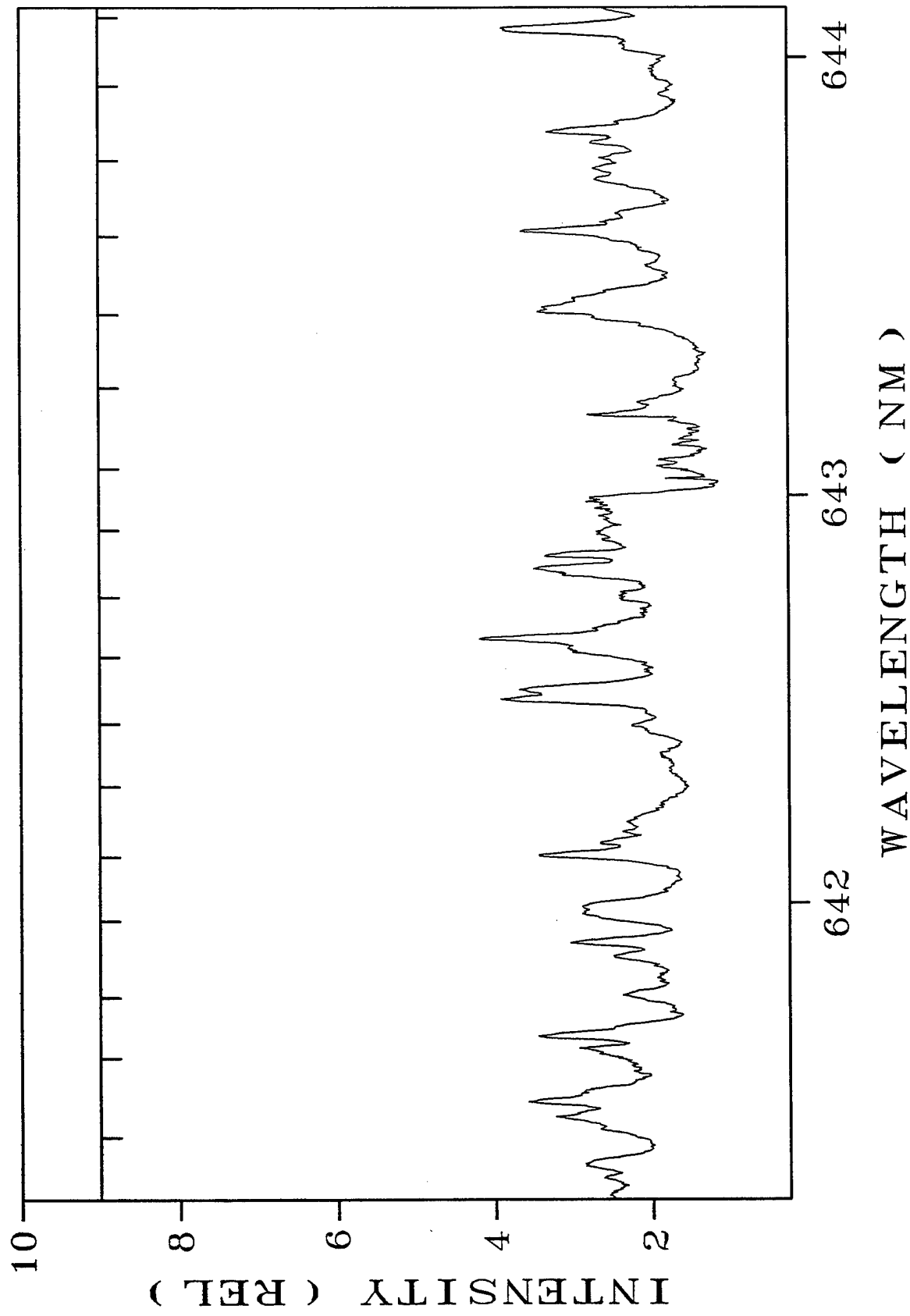

Figure B-1. (Continued).

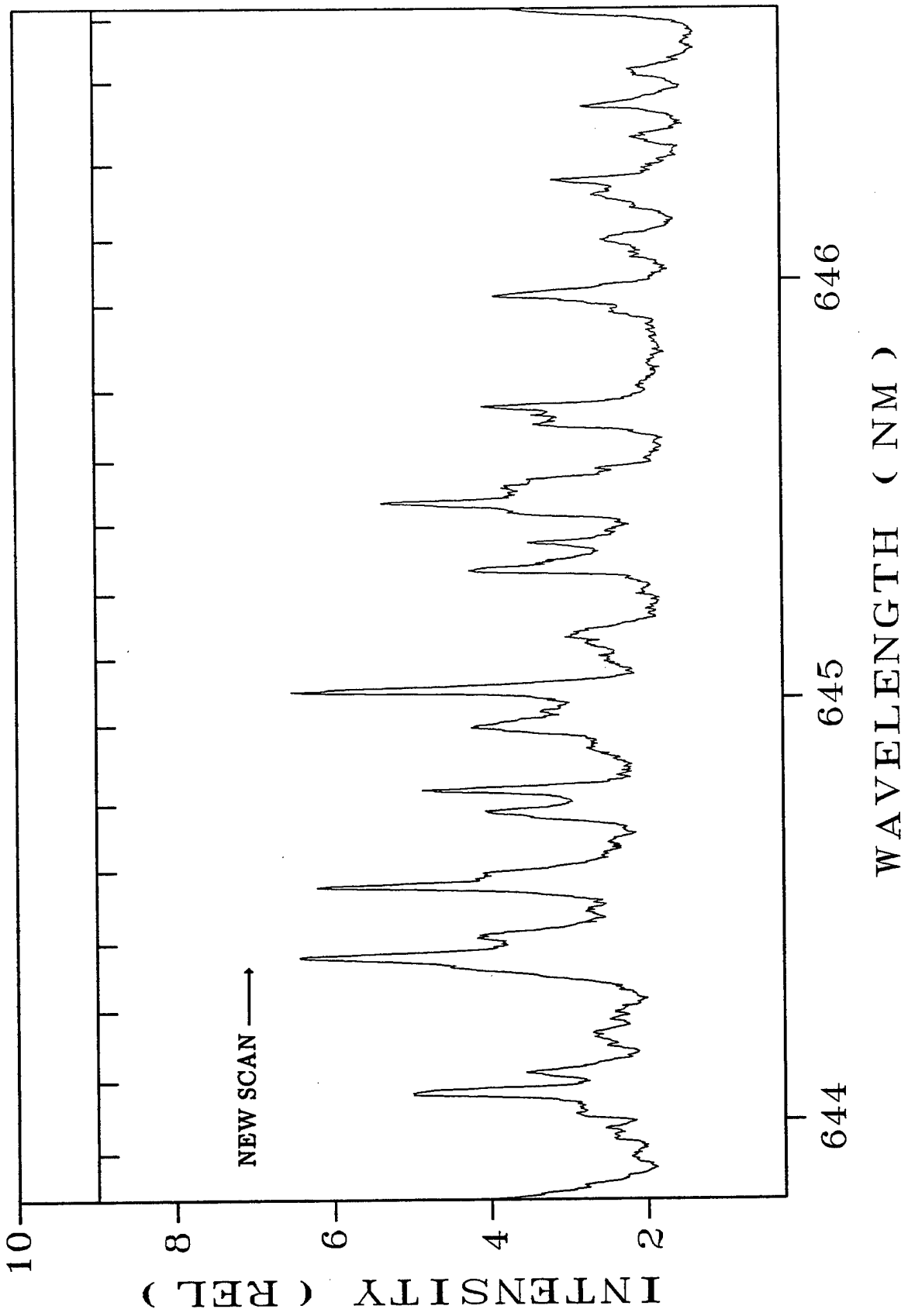

Figure B-1. (Continued).

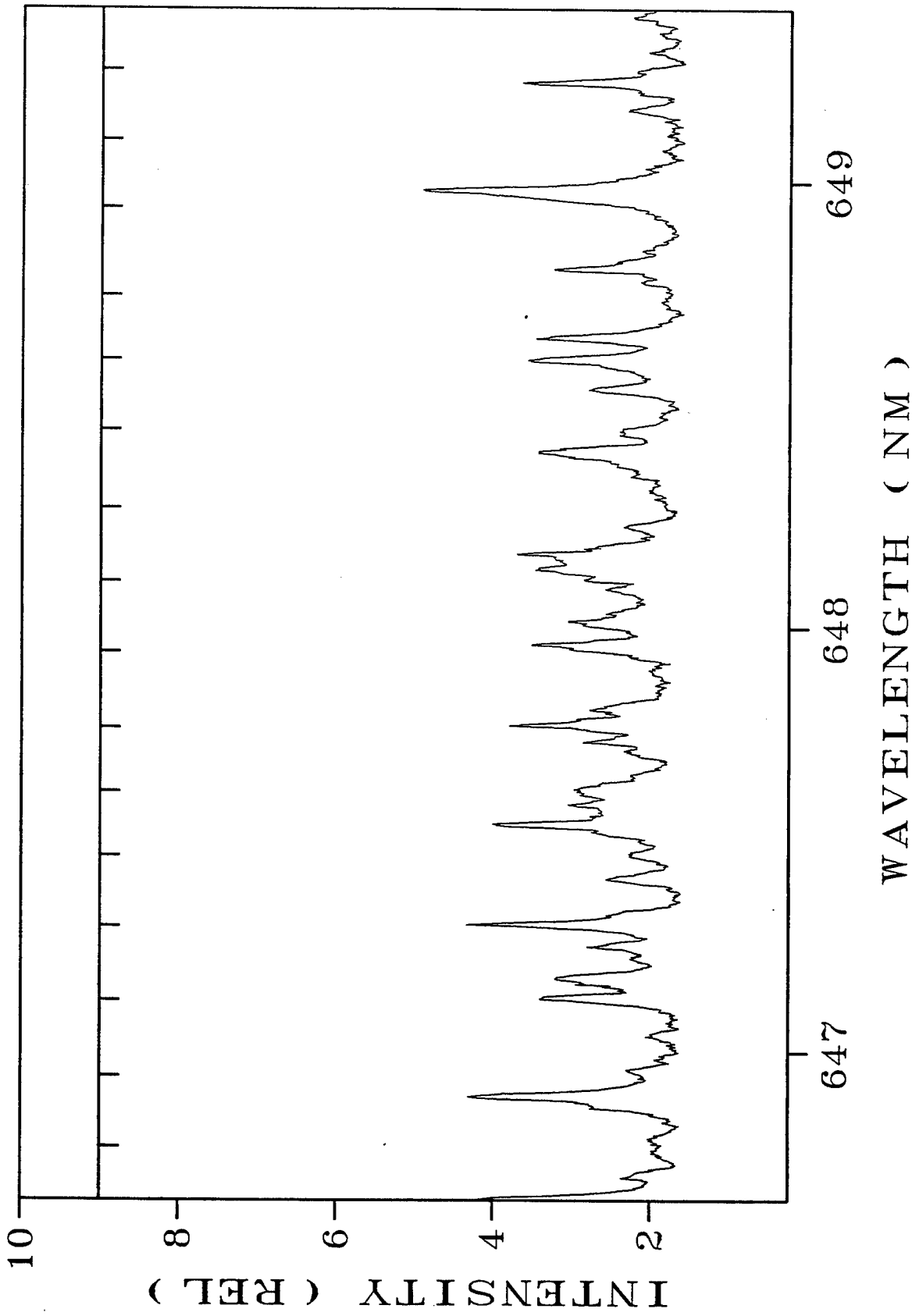

Figure B-1. (Continued).

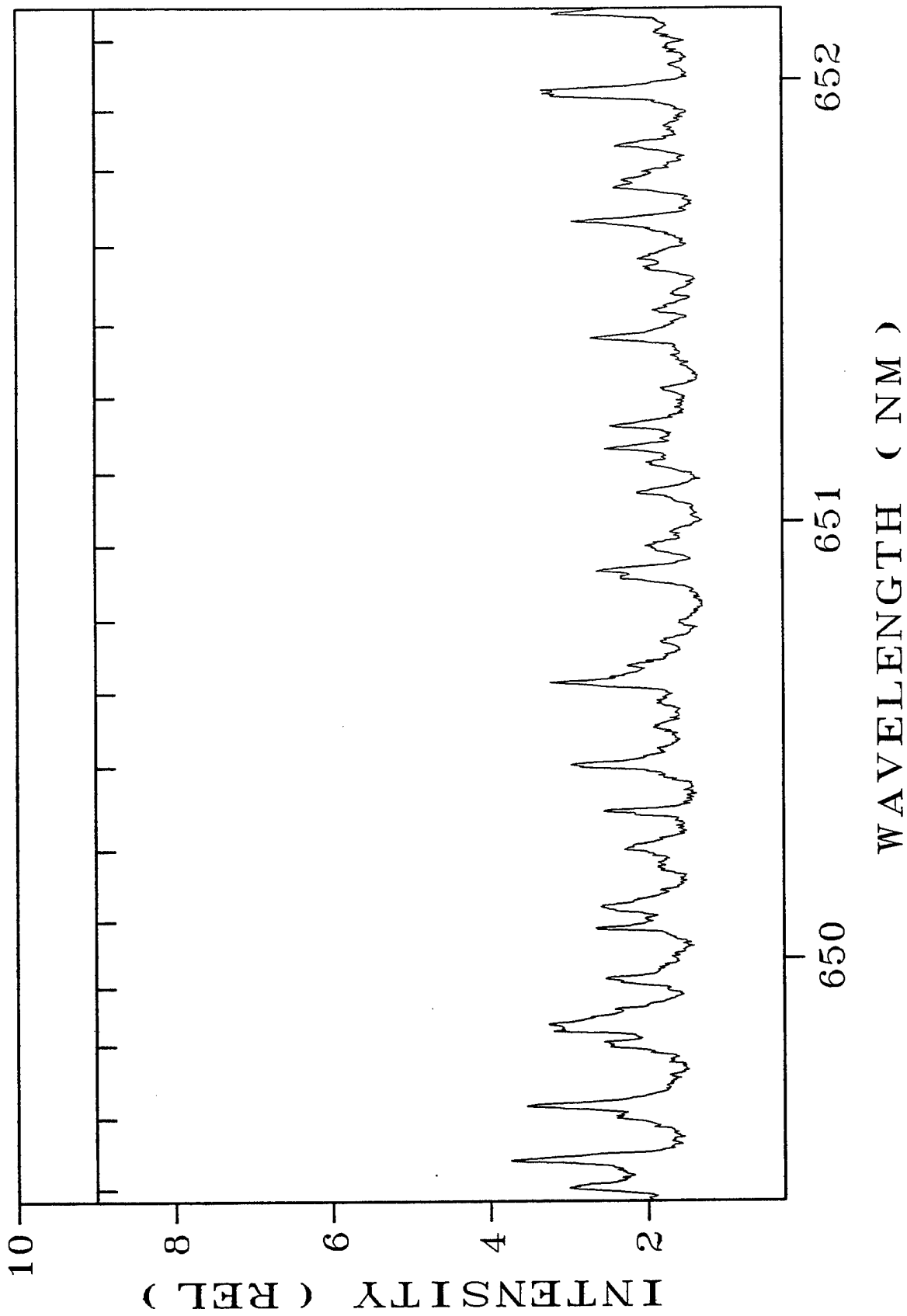

Figure B-1. (Continued).

NO. OF COPIES	ORGANIZATION
2	DEFENSE TECHNICAL INFORMATION CENTER DTIC DDA 8725 JOHN J KINGMAN RD STE 0944 FT BELVOIR VA 22060-6218
1	HQDA DAMO FDQ DENNIS SCHMIDT 400 ARMY PENTAGON WASHINGTON DC 20310-0460
1	CECOM SP & TRRSTRL COMMCTN DIV AMSEL RD ST MC M H SOICHER FT MONMOUTH NJ 07703-5203
1	PRIN DPTY FOR TCHNLGY HQ US ARMY MATCOM AMCDCG T M FISETTE 5001 EISENHOWER AVE ALEXANDRIA VA 22333-0001
1	PRIN DPTY FOR ACQUSTN HQS US ARMY MATCOM AMCDCG A D ADAMS 5001 EISENHOWER AVE ALEXANDRIA VA 22333-0001
1	DPTY CG FOR RDE HQS US ARMY MATCOM AMCRD BG BEAUCHAMP 5001 EISENHOWER AVE ALEXANDRIA VA 22333-0001
1	ASST DPTY CG FOR RDE HQS US ARMY MATCOM AMCRD COL S MANESS 5001 EISENHOWER AVE ALEXANDRIA VA 22333-0001

NO. OF COPIES	ORGANIZATION
1	DPTY ASSIST SCY FOR R&T SARD TT F MILTON THE PENTAGON RM 3E479 WASHINGTON DC 20310-0103
1	DPTY ASSIST SCY FOR R&T SARD TT D CHAIT THE PENTAGON WASHINGTON DC 20310-0103
1	DPTY ASSIST SCY FOR R&T SARD TT K KOMINOS THE PENTAGON WASHINGTON DC 20310-0103
1	DPTY ASSIST SCY FOR R&T SARD TT B REISMAN THE PENTAGON WASHINGTON DC 20310-0103
1	DPTY ASSIST SCY FOR R&T SARD TT T KILLION THE PENTAGON WASHINGTON DC 20310-0103
1	OSD OUSD(A&T)/ODDDR&E(R) J LUPO THE PENTAGON WASHINGTON DC 20301-7100
1	INST FOR ADVNCD TCHNLGY THE UNIV OF TEXAS AT AUSTIN PO BOX 202797 AUSTIN TX 78720-2797
1	DUSD SPACE 1E765 J G MCNEFF 3900 DEFENSE PENTAGON WASHINGTON DC 20301-3900
1	USAASA MOAS AI W PARRON 9325 GUNSTON RD STE N319 FT BELVOIR VA 22060-5582

NO. OF COPIES ORGANIZATION

1 CECOM
PM GPS COL S YOUNG
FT MONMOUTH NJ 07703

1 GPS JOINT PROG OFC DIR
COL J CLAY
2435 VELA WAY STE 1613
LOS ANGELES AFB CA 90245-5500

1 ELECTRONIC SYS DIV DIR
CECOM RDEC
J NIEMELA
FT MONMOUTH NJ 07703

3 DARPA
L STOTTS
J PENNELLA
B KASPAR
3701 N FAIRFAX DR
ARLINGTON VA 22203-1714

1 SPCL ASST TO WING CMNDR
50SW/CCX
CAPT P H BERNSTEIN
300 O'MALLEY AVE STE 20
FALCON AFB CO 80912-3020

1 USAF SMC/CED
DMA/JPO
M ISON
2435 VELA WAY STE 1613
LOS ANGELES AFB CA 90245-5500

1 US MILITARY ACADEMY
MATH SCI CTR OF EXCELLENCE
DEPT OF MATHEMATICAL SCI
MDN A MAJ DON ENGEN
THAYER HALL
WEST POINT NY 10996-1786

1 DIRECTOR
US ARMY RESEARCH LAB
AMSRL CS AL TP
2800 POWDER MILL RD
ADELPHI MD 20783-1145

NO. OF COPIES ORGANIZATION

1 DIRECTOR
US ARMY RESEARCH LAB
AMSRL CS AL TA
2800 POWDER MILL RD
ADELPHI MD 20783-1145

3 DIRECTOR
US ARMY RESEARCH LAB
AMSRL CI LL
2800 POWDER MILL RD
ADELPHI MD 20783-1145

ABERDEEN PROVING GROUND

2 DIR USARL
AMSRL CI LP (305)

NO. OF COPIES	ORGANIZATION
1	DEPT OF PHYSICS UNIV OF CENTRAL OKLAHOMA ATTN J A GUTHRIE EDMOND OK 73034
1	USAF PHILLIPS LABORATORY KIRTLAND AIR FORCE BASE ATTN T S BOWEN ALBUQUERQUE NM 87117

NO. OF COPIES	ORGANIZATION
	ABERDEEN PROVING GROUND
39	DIR, USARL ATTN: AMSRL-WM-P, A. W. HORST AMSRL-WM-PC, B. E. FORCH G. F. ADAMS W. R. ANDERSON R. A. BEYER S. W. BUNTE C. F. CHABALOWSKI K. P. MC-NEILL BOONSTOPPEL A. COHEN R. DANIEL D. DEVYNCK R. A. FIFER J. M. HEIMERL B. E. HOMAN A. JUHASZ A. J. KOTLAR R. KRANZE E. LANCASTER W. F. MCBRATNEY K. L. MCNESBY M. MCQUAID N. E. MEAGHER M. S. MILLER A. W. MIZIOLEK J. B. MORRIS J. E. NEWBERRY W. V. PAI R. A. PESCE-RODRIGUEZ J. RASIMAS B. M. RICE P. SAEGAR R. C. SAUSA M. A. SCHROEDER R. SCHWEITZER L. D. SEGER J. A. VANDERHOFF D. VENIZELOS W. WHREN H. L. WILLIAMS

INTENTIONALLY LEFT BLANK.

REPORT DOCUMENTATION PAGE

Form Approved
OMB No. 0704-0188

1. AGENCY USE ONLY *(Leave blank)*	2. REPORT DATE	3. REPORT TYPE AND DATES COVERED
	JUNE 1997	Final, January 1990 - December 1996

4. TITLE AND SUBTITLE

Unusual Laser Excitations (5,890-6,520 Å) of the $B^2\Sigma^+$Electronic State of CN in an Atmospheric-Pressure Flame

5. FUNDING NUMBERS

PR: 1L161102AH43

6. AUTHOR(S)

J. A. Guthrie, T. S. Bowen, W. R. Anderson, A. J. Kotlar, and S. W. Bunte

7. PERFORMING ORGANIZATION NAME(S) AND ADDRESS(ES)

U.S. Army Research Laboratory
ATTN: AMSRL-WM-PC
Aberdeen Proving Ground, MD 21005-5066

8. PERFORMING ORGANIZATION REPORT NUMBER

ARL–TR–1381

9. SPONSORING/MONITORING AGENCY NAMES(S) AND ADDRESS(ES)

10.SPONSORING/MONITORING AGENCY REPORT NUMBER

11. SUPPLEMENTARY NOTES

12a. DISTRIBUTION/AVAILABILITY STATEMENT

Approved for public release; distribution is limited.

12b. DISTRIBUTION CODE

13. ABSTRACT *(Maximum 200 words)*

The CN radical plays an important role in the chemistry of nitramine propellant flames. Diagnostic methods for detection of this radical are therefore important for studies of its role in propellant combustion experiments. In this work, CN laser induced fluorescence (LIF) in an atmospheric pressure flame was studied. The first such flame study involving observation of LIF in the strong CN B-X violet system, near 3880 Å, but with excitation using strong, fundamental dye laser outputs, near 6000 Å, is reported. Excitation at significantly longer wavelengths (smaller photon energy) than LIF observation wavelengths is unusual. Because the high intensity fundamental outputs of dye lasers may be used, these excitations could ultimately prove to be very effective diagnostic methods for this species. Subsequent investigation of the spectra has revealed that at least four distinct excitation processes, some of which involve molecular collisions, are responsible for the observed LIF as the laser is scanned in this region. The observed spectra reveal some of the unexpected effects of collisions and laser intensity on absorption and fluorescence in this molecule.

14. SUBJECT TERMS

CN radical, laser induced fluorescence, combustion, flames

15. NUMBER OF PAGES

66

16. PRICE CODE

17. SECURITY CLASSIFICATION OF REPORT	18. SECURITY CLASSIFICATION OF THIS PAGE	19. SECURITY CLASSIFICATION OF ABSTRACT	20. LIMITATION OF ABSTRACT
UNCLASSIFIED	UNCLASSIFIED	UNCLASSIFIED	UL

INTENTIONALLY LEFT BLANK.

USER EVALUATION SHEET/CHANGE OF ADDRESS

This Laboratory undertakes a continuing effort to improve the quality of the reports it publishes. Your comments/answers to the items/questions below will aid us in our efforts.

1. ARL Report Number/Author ARL-TR-1381 (Guthrie) Date of Report June 1997

2. Date Report Received _____

3. Does this report satisfy a need? (Comment on purpose, related project, or other area of interest for which the report will be used.) _____

4. Specifically, how is the report being used? (Information source, design data, procedure, source of ideas, etc.) _____

5. Has the information in this report led to any quantitative savings as far as man-hours or dollars saved, operating costs avoided, or efficiencies achieved, etc? If so, please elaborate. _____

6. General Comments. What do you think should be changed to improve future reports? (Indicate changes to organization, technical content, format, etc.) _____

CURRENT ADDRESS

_____
Organization

_____
Name E-mail Name

_____
Street or P.O. Box No.

_____
City, State, Zip Code

7. If indicating a Change of Address or Address Correction, please provide the Current or Correct address above and the Old or Incorrect address below.

OLD ADDRESS

_____
Organization

_____
Name

_____
Street or P.O. Box No.

_____
City, State, Zip Code

(Remove this sheet, fold as indicated, tape closed, and mail.)
(DO NOT STAPLE)

DEPARTMENT OF THE ARMY

OFFICIAL BUSINESS

NO POSTAGE
NECESSARY
IF MAILED
IN THE
UNITED STATES

BUSINESS REPLY MAIL
FIRST CLASS PERMIT NO 0001,APG,MD

POSTAGE WILL BE PAID BY ADDRESSEE

DIRECTOR
US ARMY RESEARCH LABORATORY
ATTN AMSRL WM PC
ABERDEEN PROVING GROUND MD 21005-5066